Dewatering Reverse Osmosis Concentrate from Water Reuse Applications Using Forward Osmosis

WateReuse Foundation

Dewatering Reverse Osmosis Concentrate from Water Reuse Applications Using Forward Osmosis

About the WateReuse Foundation

The mission of the WateReuse Foundation is to conduct and promote applied research on the reclamation, recycling, reuse, and desalination of water. The Foundation's research advances the science of water reuse and supports communities across the United States and abroad in their efforts to create new sources of high quality water through reclamation, recycling, reuse, and desalination while protecting public health and the environment.

The Foundation sponsors research on all aspects of water reuse, including emerging chemical contaminants, microbiological agents, treatment technologies, salinity management and desalination, public perception and acceptance, economics, and marketing. The Foundation's research informs the public of the safety of reclaimed water and provides water professionals with the tools and knowledge to meet their commitment of increasing reliability and quality.

The Foundation's funding partners include the U.S. Bureau of Reclamation, the California State Water Resources Control Board, the Southwest Florida Water Management District, and the California Department of Water Resources. Funding is also provided by the Foundation's Subscribers, water and wastewater agencies, and other interested organizations. The Foundation also conducts research in cooperation with the Global Water Research Coalition.

Dewatering Reverse Osmosis Concentrate from Water Reuse Applications Using Forward Osmosis

Samer Adham, MWH
Joan Oppenheimer, MWH
Li Liu, MWH
Manish Kumar, MWH

Disclaimer

CONTENTS

FIGURES

TABLES

ACRONYMS AND ABBREVIATIONS

APTS	3-Aminopropyl triethoxysilane
BSA	Bovine serum albumin
CP	Concentration polarization
DCMO	Direct contact membrane osmometer
EDA	Ethylenediamine
FO	Forward osmosis
FWR	Feed water recovery
gfd	Gallons per square foot per day
gpm	Gallons per minute
IMS	Integrated membrane system
MBR	Membrane bioreactor
mgd	Millions of gallons per day
mg/L	Milligrams per liter
μg/L	Micrograms per liter
MWCO	Molecular weight cutoff
MWH	Montgomery Watson Harza
PEG	Polyethylene glycol
PLC	Programmable logic controller
ppm	Parts per million
psi	Pounds per square inch
RO	Reverse osmosis
SC	Sodium carboxylate
SEM	Scanning electron microscopy
SFD	Specific flux decline
SS	Sodium succinamate
T-EDXA	Target energy dispersive X-ray analysis
TDS	Total dissolved solids
TMP	Transmembrane pressure
UF	Ultrafiltration
USP	United States Pharmacopeia
UV_{254}	UV absorbance at 254 nm
WWTP	Wastewater treatment plant
ZLD	Zero liquid discharge

FOREWORD

The WateReuse Foundation, a nonprofit corporation, sponsors research that advances the science of water reclamation, recycling, reuse, and desalination. The Foundation funds projects that meet the water reuse and desalination research needs of water and wastewater agencies and the public. The goal of the Foundation's research is to ensure that water reuse and desalination projects provide high-quality water, protect public health, and improve the environment.

A Research Plan guides the Foundation's research program. Under the plan, a research agenda of high-priority topics is maintained. The agenda is developed in cooperation with the water reuse and desalination communities, including water professionals, academics, and Foundation Subscribers. The Foundation's research focuses on a broad range of water reuse research topics including the following:

- Defining and addressing emerging contaminants;
- Public perceptions of the benefits and risks of water reuse;
- Management practices related to indirect potable reuse;
- Groundwater recharge and aquifer storage and recovery;
- Evaluating methods for managing salinity and desalination; and
- Economics and marketing of water reuse.

The Research Plan outlines the role of the Foundation's Research Advisory Committee (RAC), Project Advisory Committees (PACs), and Foundation staff. The RAC sets priorities, recommends projects for funding, and provides advice and recommendations on the Foundation's research agenda and other related efforts. PACs are convened for each project and provide technical review and oversight. The Foundation's RAC and PACs consist of experts in their fields and provide the Foundation with an independent review, which ensures the credibility of the Foundation's research results. The Foundation's Project Managers facilitate the efforts of the RAC and PACs and provide overall management of projects.

The Foundation's primary funding partners are the U.S. Bureau of Reclamation, the California State Water Resources Control Board, the Southwest Florida Water Management District, the California Department of Water Resources, Foundation Subscribers, water and wastewater agencies, and other interested organizations. The Foundation leverages its financial and intellectual capital through these partnerships and funding relationships. The Foundation is also a member of the Global Water Research Coalition.

This publication is the result of a study sponsored by the Foundation and is intended to communicate the results of this research project. This is a proof of concept study that focuses on exploring innovative draw solutions, commercially available forward osmosis membranes, and the feasibility of applying forward osmosis to dewater reverse osmosis concentrate.

Ronald E. Young
President
WateReuse Foundation

G. Wade Miller
Executive Director
WateReuse Foundation

ACKNOWLEDGEMENTS

Principal Investigator

Samer Adham, Montgomery Watson Harza

Project Advisory Committee

Menachem Elimelech, Yale University
Kerry Howe, University of New Mexico
Scott Irvine, U.S. Bureau of Reclamation
Rich Mills, California State Water Resources Control Board
George Tchobanoglous, University of California—Davis

EXECUTIVE SUMMARY

Reverse osmosis (RO) is an effective barrier in water production systems when removal of dissolved contaminants or salts is needed to achieve high finished water quality. RO concentrate usually comprises 10–30% of the influent for surface water and 50–75% of the influent for seawater. While coastal communities can utilize the ocean to discharge the RO concentrate, inland facilities must rely upon more problematic conventional alternatives, such as surface water or sanitary sewer discharge, evaporation ponds, deep well injection, and land applications. These options are costly, not environmentally sustainable, and increasingly difficult to permit. Thus, proper handling and disposal of the RO concentrate have become a critical environmental issue, particularly for an inland community.

A novel process of dewatering RO concentrate is forward osmosis (FO). FO is defined as the net movement of water across a selectively permeable membrane driven by a difference in osmotic pressure across the membrane (Cath et al., 2006). FO has been studied for a variety of applications such as volume minimization of sanitary landfill leachate, concentration of fruit juices, and desalting emergency water supplies for homeland security operations. The main advantage of using FO in water and wastewater treatment is the very low energy consumption rate, since no external pressure is required while rejecting a wide range of contaminants with possibly a lower membrane-fouling propensity than pressure-driven membrane processes have. The main challenges, however, exist in the manufacture of high-performance FO membranes, the selection of easily separable draw solutions with a high osmotic pressure, and the optimization of process configurations to minimize concentration polarization (CP).

As a proof of concept, this study focuses on exploring innovative draw solutions, commercially available FO membranes, and the feasibility of applying FO to dewater RO concentrate.

As a first step, **a direct contact membrane osmometer (DCMO) was designed to measure the osmotic pressures of these innovative draw solutions.** The osmotic pressure of these compounds cannot be adequately predicted on the basis of theoretical calculations because of the uncertainty in the value of physical constants needed for the calculations. Actual osmotic pressure measurement that relied on DCMO provided a basis for prediction of the performance of innovative draw solutions whose osmotic properties have not been well researched. The DCMO was calibrated up to 500 psi by using PEG-1500, and this equipment enabled us to measure the osmotic pressures in the range that is applicable to desalination.

INNOVATIVE DRAW SOLUTIONS

In this study, the selection of draw solutions used in the FO application was based on two major criteria. First, the draw solution must have a high enough osmolality to generate an osmotic pressure sufficiently greater than the osmotic pressure of the feedwater (RO concentrate). Second, the solute should be efficiently separated from water by using available technologies so that it can be recycled in the FO process. A number of innovative draw

solutions including magnetic nanoparticles, albumin, and dendrimers were investigated for their osmotic properties and recovery strategies.

Magnetic nanoparticles were evaluated in this study as a candidate draw solution. With 3 to 25 psi of measured osmotic pressure, the magnetic fluid could not provide the high osmotic driving force for dewatering RO concentrate. This deficiency can be explained by the high molecular weight and low solubility of the nanoparticles. Our measurements, however, have shown that magnetic nanoparticles may have potential if they can be appropriately synthesized. If the nanoparticles can be designed to be smaller and less viscous and endowed with a more hydrophilic surface, higher osmotic pressures may be obtainable.

It has been reported that coated magnetic nanoparticles can be captured by a high-gradient magnetic separation system by using a canister separator (Moeser et al., 2004). The magnetic nature of the nanoparticles will facilitate the removal of solute, which meets one of the important criteria for the ideal draw solution.

Another macromolecule, **albumin**, was also evaluated in this study. Albumin is a protein that has a special role in regulating the osmotic pressure balance within blood vessels. This compound, however, was not able to provide the high osmotic pressure required for dewatering RO concentrate, since only 7 psi of osmotic pressure was measured for a 30% (by weight) albumin solution. Upon heating, the albumin solution was denatured and solidified. Water could be separated from the solidified albumin, but the recovery is low.

Dendrimers are a promising osmotic medium as these macromolecules provide high osmotic pressure. Dendrimers are spheroid or globular nanostructures that are precisely engineered to carry molecules encapsulated in the interior void spaces or attached to the surface. Twenty percent of G2-pentaearythrityl sodium carboxylate dendrimer solution was measured at 330 psi with its surface ions partially dissociated. This osmotic pressure is sufficient to dewater the RO concentrate being studied.

Ultrafiltration (UF) has the potential to reconcentrate the dendrimer along with its surface ions, as a preliminary UF experiment achieved 87.3% rejection of the surface sodium ions. Additional studies need to be conducted on specially designed dendrimers with ionizable surface groups and low buffering capacity. Dendrimers with these properties would be easily adjusted to a wide range of pH values without introducing an excessive number of extra ions. The samples with adjusted pH could be ultrafiltered, and the concentration of surface ions in the filtrate could be minimized to enhance the recovery of the surface ions in the reconcentrated dendrimer solution.

COMPARISON OF FO MEMBRANES

One hollow-fiber and four flat-sheet membranes were obtained from different manufacturers for this project. The hollow-fiber membrane E came in wet as a whole RO module, and it was very difficult to convert it into a flow-through FO system. Membrane A, a flat-sheet brackish RO membrane, was tested with DCMO and proved to be too thick to use (the time to reach equilibrium was too long). Among the other three flat-sheet membranes (B, C, and D), membrane B demonstrated the greatest osmotic permeability in the FO mode (specific flux of 0.0172 gfd/psi). **Therefore, membrane B was identified as the best membrane tested in this study and was used in bench-scale FO experiments of dewatering RO concentrate.**

BENCH-SCALE FO TESTING TO DEWATER RO CONCENTRATE

Bench-scale experiments have shown that the RO concentrate was further concentrated in FO when salt (NaCl) was used as the draw solution. With the flat-sheet membrane B FO configuration, the volume of RO concentrate was reduced by 71% after 20 h of operation, achieving an overall recovery of 94% combining RO and FO processes. Scanning electron microscopy (SEM) and target energy dispersive X-ray analysis (T-EDXA) have revealed that the precipitate in the FO process was mostly calcium (99.3%) with a small amount of silica (0.7%). Low-pH cleaners could easily recover the permeability of fouled FO membrane. In this study, the fouled membrane was cleaned by using 2% citric acid (pH = 2.24), and the specific flux was recovered to 81% of the initial specific flux. Softening the RO concentrate helped to remove the hardness and silica in the feed, resulting in less specific flux decline (by 8%) than in unsoftened feed.

ECONOMIC FEASIBILITY OF APPLYING FO FOR RO CONCENTRATE MINIMIZATION

The FO process is shown to be economically feasible for RO concentrate minimization. The costs for the FO process were derived by using the bench-testing results assuming salt as the draw solution and ion exchange (IX) as the salt reconcentrating process. The recovery of the FO process is assumed to be 70% with the FO flux of 2 gfd. The detailed assumptions utilized in the economic analysis are presented in Section 3.5. As shown in Figure 3.21, the cost of implementing FO for dewatering RO concentrate before zero liquid discharge (ZLD) processing is lower than that of implementing ZLD on the entire RO concentrate stream, as substantial operational costs were saved when one utilized the FO train ($2.49/1000 gal) rather than the baseline treatment train ($3.07/1000 gal) for a 10-mgd integrated membrane system (IMS) incorporating a membrane bioreactor (MBR) and an RO process.

CHAPTER 1

INTRODUCTION

1.1 BACKGROUND

Reverse osmosis (RO) is an effective barrier in water production systems when removal of dissolved contaminants or salts is needed to achieve high finished water quality. While the installation of RO facilities has increased dramatically over the past decade (Wangnick, 2004), handling the concentrate brine produced from RO process has become an emerging issue.

RO concentrate usually comprises 10–30% of the influent for surface water and 50–75% of the influent for seawater (Adham et al., 2005). While coastal communities can utilize the ocean to discharge the RO concentrate, inland facilities must rely upon more problematic conventional alternatives, such as surface water or sanitary sewer discharge, evaporation ponds, deep well injection, and land applications (Mickley, 2001). These options are costly, not considered environmentally sustainable, and becoming increasingly difficult to permit (AWWA, 2004). The industry has therefore been searching for cost-effective and environmentally sensitive alternatives for RO concentrate handling.

A novel process for dewatering RO concentrate is forward osmosis (FO). Osmosis is defined as "the net movement of water across a selectively permeable membrane driven by a difference in osmotic pressure across the membrane" (Cath et al., 2006). Osmosis is a ubiquitous process in nature and has been extensively studied and utilized in engineered systems. In RO, a concentrated feed is "pushed" through a semipermeable membrane by applying an external pressure sufficient to overcome the osmotic pressure of the feed. FO is the opposite of RO (Figure 1.1) and is a direct application of the osmotic principle. When solutions of different solute concentrations are separated by a semipermeable membrane, the solvent (i.e., water) will move across the membrane from the lower-solute-concentration side to the higher-concentration-solute side (i.e., "draw solution"). The driving force for this movement is the osmotic pressure gradient across the membrane caused by the differences in solute concentrations.
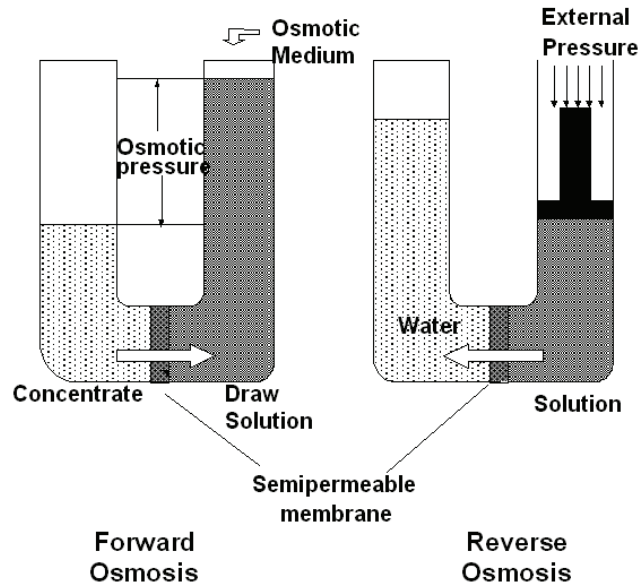
Figure 1.1. Comparison of FO and RO.

The main advantage of using FO in water and wastewater treatment is lower energy consumption because no external pressure is required. The FO process may also demonstrate a lower membrane-fouling propensity than pressure-driven membrane processes do. The main challenges, however, exist in the manufacture of high-performance FO membranes and the selection of easily separable draw solutions with a high osmotic pressure (Cath et al., 2006). In addition, the water flux in the FO process is often much lower than the flux expected from the bulk osmotic pressure difference and membrane permeability. This is often attributed to concentration polarization (CP), especially internal CP (McCutcheon et al., 2006). Consequently, the hydraulic configurations of the FO process need to be optimized to minimize CP and membrane fouling.

FO has been studied for a variety of applications such as volume minimization of sanitary landfill leachate (York et al., 1999; Osmotek, Inc.), concentration of fruit juices (Petrotos et al., 1998), desalting (McGinnis, 2002; Cath et al., 2006; McCutcheon et al., 2005; McCutcheon et al., 2006) and emergency water supply equipment for homeland security operations (D. Cohen). So far, few studies about applying FO to dewater RO concentrate have been reported.

As a proof-of-concept study, this report summarizes initial feasibility data on the application of FO to minimize the concentrate from RO process. It also contributes to the knowledge base of novel draw solutions and high-performance FO membranes.

1.2 OBJECTIVES

The major project objectives were:

- o To investigate the viability of utilizing FO for dewatering RO concentrate.

- o To investigate alternate membrane configurations for FO applications.

- o To investigate innovative draw solutions and compare them with baseline draw solutions.

- o To investigate the economic feasibility of dewatering RO concentrate by using FO.

CHAPTER 2

MATERIALS AND METHODS

2.1 TESTING SITES

This project involved the use of two test locations. The RO concentrate was generated for the study from an RO pilot system installed at a wastewater facility in New Mexico. The FO bench-scale tests for dewatering the RO concentrate were conducted at the MWH Research Center and Fabrication Facility in California.

2.1.1 Pilot Testing Site Description

The RO concentrate for this project was generated from a pilot system installed at the City of Rio Rancho Wastewater Treatment Plant 2 (WWTP No. 2) located in Rio Rancho, NM. The integrated membrane system (IMS) pilot consisted of a membrane bioreactor (MBR), a programmable logic controller (PLC) unit, and a trailer-mounted RO system installed at the western edge of the treatment plant's anoxic basins.

The feed water to the IMS pilot treatment train is WWTP No. 2's prescreened, degritted raw wastewater, which was passed through a grinder and an additional prescreen before being fed to the MBR unit. The Kubota MBR unit consisted of a denitrification zone, prenitrification zone, and aerobic tank. MBR effluent from the aerobic tank passed through the pilot unit auxiliary skid to the RO feed tank. The RO feed was then pumped with a submersible pump to the pilot unit RO trailer. As pretreatment, the feed was dosed with chloramine and passed through a 5-µm RO prefilter (Enviroquip, Austin, TX) and then passed through the RO pilot, and the concentrate was collected for subsequent bench-scale testing. For this study the RO pilot system was operated at 80% feed water recovery from a 2-1 pressure vessel array. An illustrative schematic of the treatment train can be seen in Figure 2.1.
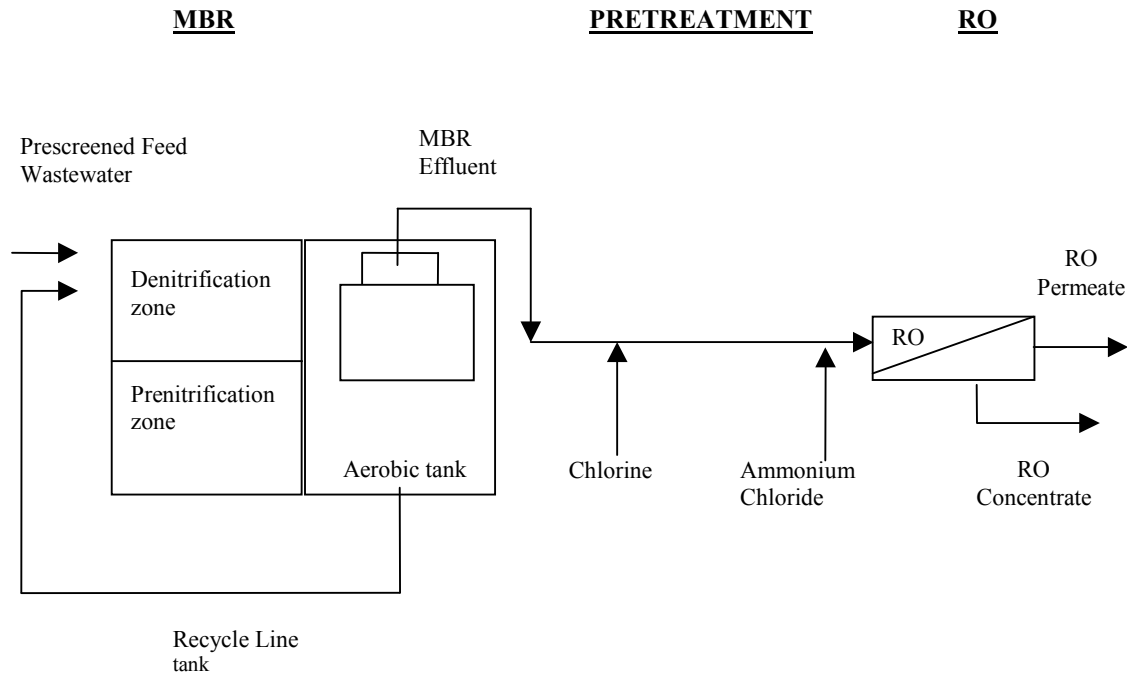
Figure 2.1. Process flow diagram of the pilot train at Rio Rancho WWTP No. 2.

2.1.2 Bench Testing Site Description

Bench-scale testing was conducted at the MWH Research Center and Fabrication Facility in Monrovia, CA. The RO concentrate collected from the IMS pilot testing site at Rio Rancho, NM, was shipped in drum containers to Monrovia, CA. Once received, the water was stored at 4 ^{o}C throughout the study to inhibit biological activity. However, to minimize any changes in the water composition, the experiments were scheduled to start immediately after receipt of the water.

2.2 DRAW SOLUTIONS

In this study, the selection of draw solutions used in the FO application was based on two major criteria. First, the draw solution must have a high enough osmolality to generate an osmotic pressure sufficiently greater than the osmotic pressure of the feedwater (RO concentrate). This is best achieved by utilizing substances with high solubility and low molecular weight (Cath et al., 2006). Second, the solute should be efficiently separated from water by using available technologies so that it can be recycled in the FO process.

A number of draw solutions including sodium chloride (NaCl), magnetoferritin nanoparticles, dendrimers, and albumin were evaluated. Table 2.1 summarizes the physical properties of tested draw solutions.

Table 2.1. Physical Properties of Tested Draw Solutions

	Mol Wt (g/mol)	Viscosity (cp), at 20~24 °C, 0.1 MPa	Maximum Concn (wt%)	Surface Groups
Sodium chloride	58.5	1.005 at 1 mol/L[a]	26	—
Magnetic nanoparticle	1.7×10^5 – 7.8×10^6	NA	45	Quaternary ammonium; PEG-5000
Dendrimers G2-EDA G3-EDA G5-EDA G2-pentaearythirityl	5.2×10^3 1.1×10^4 4.4×10^4 4.0×10^3	NA	20–45	16 of SS[c] 32 of SS 128 of SS 24 of SC[d]
Bovine serum albumin (BSA)[e]	6.6×10^4	1.6 at 0.001 mol/L[b]	30	—

[a] Kestin and Shankland, 1984.

[b] Tu and Breedveld, 2005.

[c]SS, sodium succinamate.

[d]SC, sodium carboxylate.

[e]BSA, bovine serum albumin.

Sodium chloride
The USP-grade sodium chloride obtained from Morton Salt (Chicago, IL) meets the standards of the United States Pharmacopeia, and the purity theoretically exceeds 99.95% sodium chloride. As shown in Table 2.1, salt has excellent properties as an osmotic agent including low molecular weight (58.5 g/mol), low viscosity (~1 cp for a 1-mol/L solution), and high solubility (up to 26% in water). In this study, salt was used as a baseline from which to design and evaluate real-world application of our flow-through system for concentrate dewatering by FO.

Magnetic nanoparticles
The nanoparticles for this testing were synthesized at the Center for Bioinspired Materials, Montana State University, Bozeman. The synthesis of nanoscale magnetic particles was achieved by using a high-pH precipitation of Fe(II) and Fe(III) salts from aqueous solution. After this initial synthesis, additional functional groups were added to the surface in order to increase the charge density on each nanomagnetic particle. Surface exposed OH groups on the exterior of the magnetite particles were allowed to react with 3-aminopropyl triethoxysilane (APTS) under acidic conditions (pH 4). The resultant particles were separated from unreacted APTS by exhaustive dialysis and concentrated by high-speed centrifugation. In a modification of this reaction scheme, designed to achieve better draw solution characteristics, the initial magnetite nanoparticles were reacted with a triethoxysilane derivative of polyethylene glycol (PEG) under similar reaction conditions to generate magnetic particles with a PEG coating. In this study, the size of magnetic nanoparticles range from 7 to 25 nm in diameter, while concentrations go up to 45% by weight (Table 2.1). There are no viscosity data available on the customized magnetic nanoparticles, although according to visual observation, the magnetic fluid was highly viscous.

Dendrimers

Dendrimers are spheroid or globular nanostructures that are precisely engineered to carry molecules encapsulated in the interior void spaces or attached to the surface (Dendritic Nanotechnology, Inc., 2006). These macromolecules consist of a highly branched tree-like structure (identical to fractals) linked to a central core though covalent bonds. Dendrimers are constructed through a set of repeating chemical synthesis procedures that build up from the molecular level to the nanoscale region. The number of synthesis cycles that the dendrimer has gone through is called generation.

A schematic illustration of the growth of a dendrimer through different generations is provided in Figure 2.2. The dendrimer diameter increases linearly with the growth of generation, whereas the number of surface groups increases geometrically.
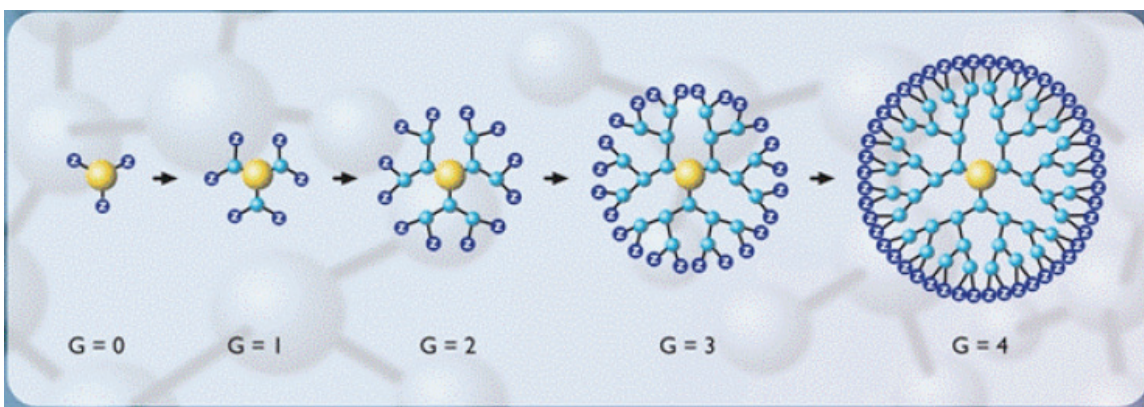
Figure 2.2. Growth of dendrimer from generation (G) zero to generation four (courtesy of Dendritic Nanotechnology).

In this study, four types of dendrimers were obtained from Dendritic Nanotechnology, Mt. Pleasant, MI (Table 2.1). They are ethylenediamine (EDA) core dendrimers with G2, G3, and G5 structures and sodium succinamate (SS) terminal groups and a pentaearythirityl core dendrimer with a G2 structure and sodium carboxylate (SC) terminal groups. The molecular weights of the tested dendrimers ranged from 4027 to 10,804 g/mol. The maximum concentration of the dendrimer solution was up to 45% by weight.

Albumins

The bovine serum albumin (BSA) tested in this study was minimum 98.0% pure (Mallinckrodt Baker, Inc., Phillipsburg, NJ). The BSA has a molecular weight of approximately 66,000 g/mol. Albumin is a protein that has a special role in regulating the osmotic pressure balance within blood vessels (Singh-Zocchi et al., 1999). One-millimole-per-liter albumin solution has a viscosity of 1.6 cp. As shown in Table 2.1, up to 30% (by weight) of albumin solution was tested.

2.3 MEMBRANES TESTED

The ideal FO membrane should have the following characteristics (McCutcheon et al., 2005; Cath et al., 2006):

- o A thin membrane with minimum support layer for lower CP and higher permeate production.
- o Membrane with high salt rejection.
- o Membranes with a hydrophilic surface for operational ease during the FO process. A hydrophobic membrane could lead to trapping of air between the feed and draw solution streams and reduction of the effective membrane area.

In this study, the selection of FO membranes was based on the above criteria in order to have the best chance of demonstrating high permeate production in the FO mode. Four flat-sheet and one hollow-fiber membranes were obtained from four manufacturers for this project. The characteristics of these membranes are summarized in Table 2.2.

Table 2.2. Characterization of Tested Membranes

	Vendor	Module	Thickness (μm)	Materials	Reported Salt Rejection
Membrane A	Hydranautics	Flat sheet	170	Sulfonated polyether sulfone	50%
Membrane B	Hydration Technologies	Flat sheet	130	Cellulose triacetate	95%
Membrane C	Hydration Technologies	Flat sheet	200	Cellulose triacetate	96%
Membrane D	Saehan	Flat sheet	100	Polyamide	>99%
Membrane E	Toyobo	Hollow fiber	40–50	Cellulose triacetate	>99%

2.4 EXPERIMENTAL SETUP

2.4.1 DCMO Setup

A custom-designed direct contact membrane osmometer (DCMO) was used to measure the osmotic pressures of the innovative draw solutions. The DCMO device consists of a smaller stainless steel chamber containing the draw solution centrally located within a larger water bath containing the standard solution. The bottom of the draw solution chamber is connected to a pressure transducer (0–500 psi, 4–20 mA; GE Druck, Billerica, MA). This transducer has an output of 4–20 mA (representing pressure) that was recorded in 20-s intervals with a data acquisition card and ACR Trend Reader software (ACR Systems, Inc., Surrey, BC, Canada). A photograph of the DCMO is provided in Figure 2.4.

This osmometer was designed and constructed by utilizing the principle of osmotic stress. In each test, a standard solution with known osmotic pressure was placed in the bath (

Figure 2.3). The draw solution to be tested was injected into the fluid chamber by using a syringe and needle. A piece of semipermeable membrane (permeable to water but impermeable to the solutes in the draw solution and bath solution) was wetted with the bath solution, and was laid down on the test solution meniscus while we ensured that air bubbles were not trapped in the fluid chamber. A stainless steel wire mesh was laid on top of the membrane to prevent it from bulging when pressurized, and the lid of the device was tightened against an O-ring seal. The DCMO was then placed in the bath solution. This setup allowed water to flow from the standard solution (of low osmotic strength) to the draw solution in the chamber due to the osmotic pressure difference. The resulting pressure inside the chamber was measured as a function of time until it did not change significantly, which indicated that equilibrium had been reached. This equilibrium pressure was recorded as the osmotic pressure difference between the standard solution and the osmotic agent. This method of directly measuring osmotic pressure has been reported by Chahine et al. (2005).
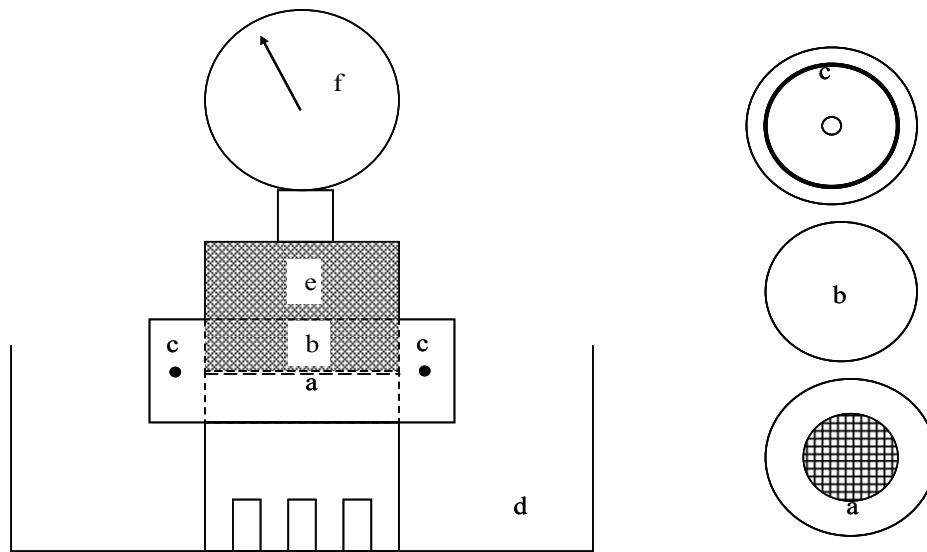
(a) mesh
(b) membrane
(c) o-ring
(d) standard solution (in bath)
(e) draw solution (in chamber)
(f) pressure gauge (or transducer)

Figure 2.3. DCMO setup.

(a) Top view of the DCMO device with a pressure gauge. (b) Tested solutions are injected into the fluid chamber, and the resulting pressure is measured at the pressure port.

Figure 2.4. Photograph of DCMO.

2.4.2 FO Setup

Three different membrane configurations (flat sheet, spiral wound, and hollow fiber) were considered for this testing. The hollow-fiber membrane E, however, came in wet as a whole module and was very difficult to convert to a flow-through FO setup. As a result, the hollow-fiber configuration was eliminated from the following evaluation, and only the flow-through systems using flat-sheet and spiral-wound membranes are presented.

Flat-Sheet Setup

A schematic diagram of the flat-sheet FO setup is shown in Figure 2.5. The three major components of this setup are the cross-flow membrane cell, the draw solution flow loop, and the RO concentrate flow loop.

The membrane component is where the actual transport of the water occurred from the concentrate into the draw solution. The custom-designed membrane cell has a flow channel on both sides of the membrane. Each channel has dimensions of 2, 146, and 95 mm for channel height, length, and width, respectively. Feed and permeate spacers (0.864 mm) were placed within both channels to promote turbulence and enhance mass transport. Centrifugal pumps (model AC-2CP-MD; March Manufacturing, Inc., Glenview, IL) were used to pump the solutions. The draw solution flowed on the active layer of the membrane and the feed on the permeate side. Concurrent flow was used to minimize the shear force on the membrane. For most testing conditions, the cross-flow rate for the feed and the draw solutions were both maintained at 1.0 L/min (equivalent to 15.4 cm/s).
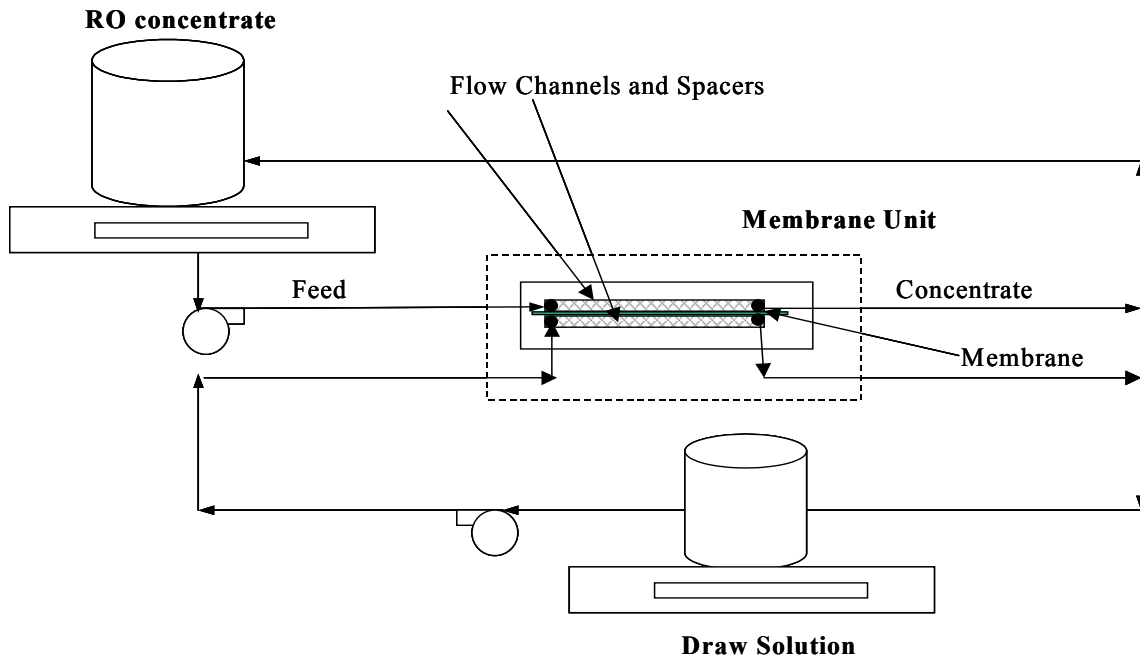
Figure 2.5. Schematic diagram of the flat-sheet FO setup.

The weight of the feed solution (in some cases the draw solution) was monitored over time by using a scale (model TR15RS; Ohaus Corp., Pine Brook, NJ) in order to determine the volume of water transported through the membrane and to calculate the membrane flux. The system was operated in semibatch mode, and the draw solution was injected once. As FO occurred, the draw solution became diluted and the change in water flux with time was recorded. The conductivity of the draw and feed solutions were monitored throughout the experiment by using a HACH (Loveland, CO) SensION5 portable conductivity/total dissolved solids (TDS) meter. From the conductivity versus salt concentration calibration curve (Section 2.6.2), the concentration of salt in the draw and feed solutions was determined, and the bulk osmotic driving force was calculated.

As the RO concentrate is dewatered, an increase in concentration of the sparingly soluble salts can lead to precipitation. A solution of 2% citric acid was used to clean the fouled membrane and recover the water flux. The cleaning solution was utilized in a cleaning bath not shown in Figure 2.5.

Spiral-Wound Setup

To evaluate the FO process in treating a high volume of RO concentrate, membrane B was spiral wound by the vendor with a high surface area of 1.5 m^2. The spiral-wound membrane was operated with only one stream (the draw solution) flowing under controlled flow velocity tangential to the membrane. With this membrane element, the dewatering of feed RO concentrate was performed in a batch mode, as the membrane was soaked in the feed tank and the draw solution was pumped through the loop. A schematic diagram of the spiral-wound setup is shown in Figure 2.6. This experiment was conducted as a quick comparison with the flat-sheet setup. In order to build a "true" flow-through system, however, flow on the feed side needs to be introduced and the hydraulic conditions need to be optimized.
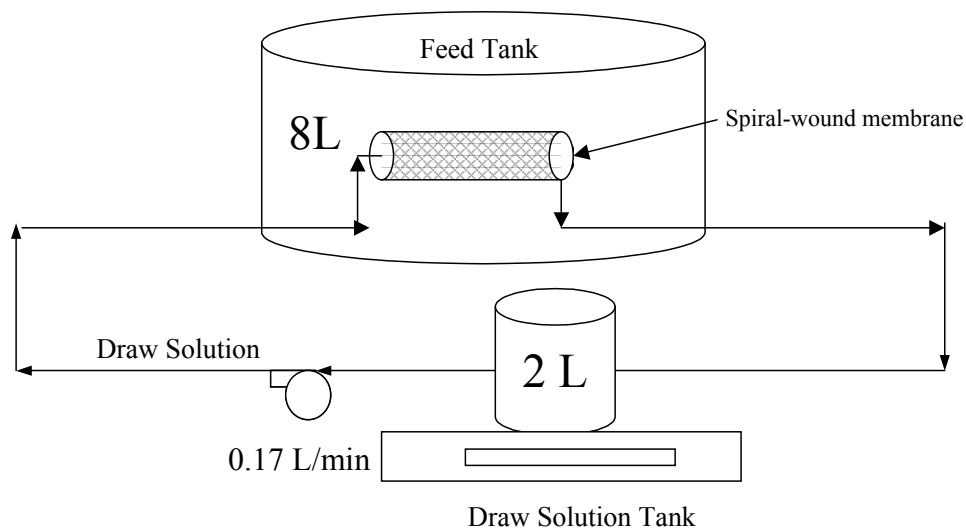
Figure 2.6. Schematic diagram of the spiral-wound FO setup.

2.5 EXPERIMENTAL PROCEDURES

All the experiments were conducted at room temperature (22 $\pm$ 2 $^{\circ}$C). The objectives of this study were investigated by conducting a series of tests in the order described below.

2.5.1 Characterization of Draw Solutions

This test was used to determine the suitability of the draw solutions selected for the study. First, the osmotic pressures of the draw solutions were determined. For innovative draw solutions whose osmotic properties are unknown, the DCMO was used to measure the osmotic pressure difference from different osmotic agents.

To validate the DCMO, the osmotic pressure of PEG-1500 (PEG with a molecular weight of 1500 Da) was measured at concentrations of 50, 100, 150, and 200 g/L with deionized water utilized as the standard solution in the bath. The osmotic pressures of 300, 400, and 450 g/L of PEG-1500 were measured by using 200, 300, and 400 g/L of PEG-1500 as the standard solution in the bath. The measured osmotic pressures were compared with published data (Cohen and Highsmith, 1997) to validate the accuracy of the DCMO.

The osmotic pressure of the magnetic nanoparticles was measured by using deionized water as the standard solution in the bath for a range of concentrations (5 to 45%). Measurements of BSA pressure were conducted for concentrations of 150 and 300 g/L (with deionized water as the standard solution in the bath). The osmotic pressure of dendrimers was measured with different generations at concentrations of 5% (w/w) and 20% (w/w) with deionized water as the standard solution in the bath.

If a draw solution demonstrated an osmotic pressure significantly higher than that of the RO concentrate solution used in this study, this draw solution was considered promising and subsequent study on the removal of the solute from this draw solution was conducted.

2.5.2 Selection of FO Membranes

FO membranes were short-listed for additional testing based on some of the criteria described for ideal FO membranes in Section 2.3. Preliminary screening of FO membranes was conducted by using the DCMO apparatus. The time for the DCMO to reach equilibrium was a function of the water transport rate, which was probably affected by the permeability of the DCMO membrane. The different FO membranes were tested by using the DCMO, and the time for the draw solution to reach osmotic equilibrium was recorded. The membranes requiring significantly longer time to reach equilibrium were eliminated from further study.

The remaining membranes were tested for permeability in both RO and FO flow-through setups. The membrane with the best productivity (flux rate) in the FO mode was used for further experiments.

2.5.3 Flow-Through Experiments

Table 2.3 summarizes all the testing conditions of the flow-through experiments. For each testing run, the experimental conditions are detailed as follows:

Table 2.3. Summary of Flow-Through Testing Conditions

Run. No.	Description	Membrane	Feed Solution	Draw Solution	Velocity (cm/s)
Run 1	Permeability and salt rejection test	Fresh membranes B,C, and D	2 L of deionized water	1 L of 30-g/L and 50-g/L NaCl	15.4
Run 2	FO with RO concentrate	Best membrane identified in Run 1, fresh	2 L of RO concentrate	1 L of 100-g/L NaCl; 2 L of 50-g/L NaCl	15.4
Run 3	FO with softened RO concentrate	Same as Run 2, fresh	2 L of softened RO concentrate	1 L of 100-g/L NaCl	15.4
Run 4	FO with membrane cleaning	Same as Run 2, used and cleaned	2 L of RO concentrate	1 L of 100-g/L NaCl	15.4
Run 5	FO with cartridge	Cartridge; membrane B	8 L of RO concentrate	2 L of 100-g/L NaCl	2.6

Permeability and Salt Rejection Tests of Flat-Sheet Membranes

The flat-sheet membranes were characterized in terms of specific flux and rejection in both RO and FO flow-through modes. The membrane demonstrating the greatest osmotic permeability in the FO mode was identified as the best membrane and was used in subsequent experiments.

In the RO permeability tests, deionized water was the feed, and flux data were collected under different operational pressures. Salt rejection tests in the RO mode were conducted with 2500 mg of NaCl/L as the feed solution. Salt rejections were calculated by measuring the conductivity of the feed and permeate by using a HACH SensION5 portable conductivity /TDS meter. From a conductivity versus salt concentration calibration curve, the concentration of salt in the permeate solution was determined, and salt rejection was calculated.

In the FO permeability tests, deionized water was used as the feed and NaCl was used as the draw solution for providing the driving force. Osmotic flux data were collected for NaCl draw solutions with concentrations of 30 and 45 g/L. Salt rejections of the membranes tested in the FO mode were calculated by measuring the conductivity of the feed solution. The trace amount of salt passing through the membrane from the draw solution (in the reverse direction of water) contributed to the conductivity of the feed solution.

FO Testing with RO Concentrate

The flat-sheet setup was tested by using actual RO concentrate from the Rio Rancho pilot testing site to determine the applicability of the FO process. One liter of 100-g/L NaCl (or 2 L of 50-g/L NaCl) was used as the draw solution to dewater 2 L of RO concentrate. The weight of RO concentrate was monitored over time to calculate the water flux. Conductivity of the RO concentrate and NaCl was recorded as a surrogate parameter for continuously monitoring osmotic pressure during the experiments (Section 2.6.2). Elemental analysis of Na, Mg, B, Sr, Ca, and Si was performed on the draw and feed solutions in order to calculate the membrane rejection of these specific elements.

As the concentrate becomes dewatered, the sparingly soluble salts in the feed might precipitate. At the end of the experiment, the membrane cell was opened, and any precipitate on the membrane surface was collected for analysis. The morphology and composition of this precipitate were analyzed by Professional Water Technologies, Inc. (Oceanside, CA) by using scanning electron microscopy (SEM) and target energy dispersive X-ray analysis (T-EDXA).

FO Testing with Softened RO Concentrate

The RO concentrate contained a significant amount of TDS, predominantly comprised of cations and anions. The RO recovery of the IMS pilot in Rio Rancho was limited to 80% due to the concentrations of silica and hardness in the feedwater (MWH, 2006). These compounds were suspected to be contributors toward limiting the recovery of the FO process, albeit at a much higher overall recovery than what was observed at the RO pilot facility because of the lack of applied pressure. To address this issue, a chemical softening process was implemented for some of the flow-through experiments in order to remove hardness ions and silica and determine the impact on the recovery of the FO process.

For flow-through experiments with presoftening, the feed solution (RO concentrate) was pretreated by using the following procedures. First, the pH of the RO concentrate was increased to 11, and then 300 mg of dolomitic lime/L and 100 mg of ferric chloride/L were added to the solution. After addition of chemicals, jar tests (Phipps and Bird, Richmond, VA) were conducted according to the following sequence: 1 min of rapid mixing at 100 rpm, 30 min of slow mixing at 30 rpm, and 1 h of settling. The supernatant was then utilized as the feed solution to the FO setup by using 1 L of 100-g/L NaCl as the draw solution to dewater 2 L of the presoftened RO concentrate.

FO Testing with Membrane after Chemical Cleaning

To investigate if the flux decline of FO membranes can be recovered by using regular chemical cleaning, a series of experiments was conducted. After 22 h of continuous operation, the membrane in the FO cell was chemically cleaned. The membrane was soaked in 2% of citric acid bath for 20 min and placed back in the FO cell. A new trial of FO was started with 1 L of 100-g/L NaCl as the draw solution to dewater 2 L of RO concentrate. The osmotic flux was monitored over time.

FO Testing with Spiral-Wound Membrane

The FO testing with spiral-wound membrane F was conducted to explore the possibility of scaling up this dewatering process to a real-world application. Eight liters of RO concentrate was dewatered by 2 L of 100-g/L NaCl solution at a flow rate of 0.17 L/min (equivalent to 2.6 cm/s of cross-flow velocity). The experiment lasted about 5 h as the draw solution was quickly diluted and as flux significantly dropped.

2.6   CALCULATIONS IN BENCH-SCALE TESTING

2.6.1   Calculation of Osmotic Pressure

Osmotic pressure calculations for RO concentrate and NaCl solutions were performed by using the van't Hoff equation.

$$\Pi = mRT \qquad\qquad\qquad \text{(Equation 2-1)}$$

Where, Π = osmotic pressure, bars
m = molar concentration of all solutes (moles/liter), in the case of multiple ionizable solutes, $m = \sum_{i=1}^{m} m_i$
R = universal gas constant, 0.083145 L•bar/moles•K
T = temperature in kelvins

The osmotic pressure of an RO concentrate was dependent upon its specific ionic composition, since compounds with lower molecular weights produced higher osmotic pressure for the same mass of solute.

For high concentrations of NaCl draw solution (30 to 100 g/L) used in this study, the van't Hoff equation is not adequate because it is derived by using dilute solution assumptions. To account for the assumption of diluteness, the nonideal behavior of concentrated solutions, and the compressibility of liquid at high pressure, a nonideality coefficient (osmotic coefficient φ) is incorporated into Equation 2-1.

$$\Pi = \varphi\, mRT \qquad\qquad\qquad \text{(Equation 2-2)}$$

Where φ = osmotic pressure coefficient, unitless

The osmotic pressure coefficient φ can be obtained from MWH, 2005 (Figure 17-10, page 1449).

Osmotic pressure (Π) is also expressed in the unit of pounds per square inch (psi). The conversion between the two units is

Osmotic pressure (Π) = 1 bar = 14.5 psi   (Equation 2-3)

2.6.2   Calculation of Osmotic Flux

In the forward osmotic setup, the osmotic flux was measured by using changes in the weight of the draw solution over time as calculated with the following relationship:

Flux (J) = $\Delta W/(\rho_w\ A\ \Delta t)$ (Equation 2-4)

Where J = membrane flux (m^3/m^2·s)
ΔW = change in weight (kg) in time period Δt(s)
ρ_w = density of water (kg/m^3)
A = membrane area (m^2)
Δt = change in time (s)

Flux (J) is also expressed in the unit of gallons per square foot per day (gfd). The conversion between the two units is

Flux (J) = 1 m^3/m^2·s = 2.12×10^6 gfd

Specific membrane flux (J_{sp}) was calculated by dividing the flux with the driving force, in this case, the osmotic pressure difference across the membrane.

Specific flux (J_{sp}) = $J/\Delta\Pi$ (Equation 2-5)

Where J_{sp} = specific membrane flux (gfd/psi)
J = membrane flux (gfd)
$\Delta\Pi$ = osmotic pressure difference across the membrane (psi)

Normalized specific flux ($J_{sp,t}/J_{sp,0}$) was calculated by dividing the specific flux at time t ($J_{sp,t}$) with the initial specific flux ($J_{sp,0}$) at time zero.

Normalized specific flux = $J_{sp,t}/J_{sp,0}$ (Equation 2-6)

Where $J_{sp,t}$ = specific membrane flux (gfd/psi) at time = t
$J_{sp,0}$ = initial specific membrane flux (gfd/psi) at time = 0

As FO occurred, the draw solution got diluted over time and the osmotic driving force $\Delta\Pi$ dropped. To capture the change in osmotic pressure driving force, the conductivity of the draw and feed solutions were monitored through the experiment. As shown in Figure 2.7, a calibration curve of conductivity versus salt concentration was established at room temperature in this experiment.

*NaCl concentration (g/L) = 0.688 * conductivity (mS/cm)*

(Equation 2-7)
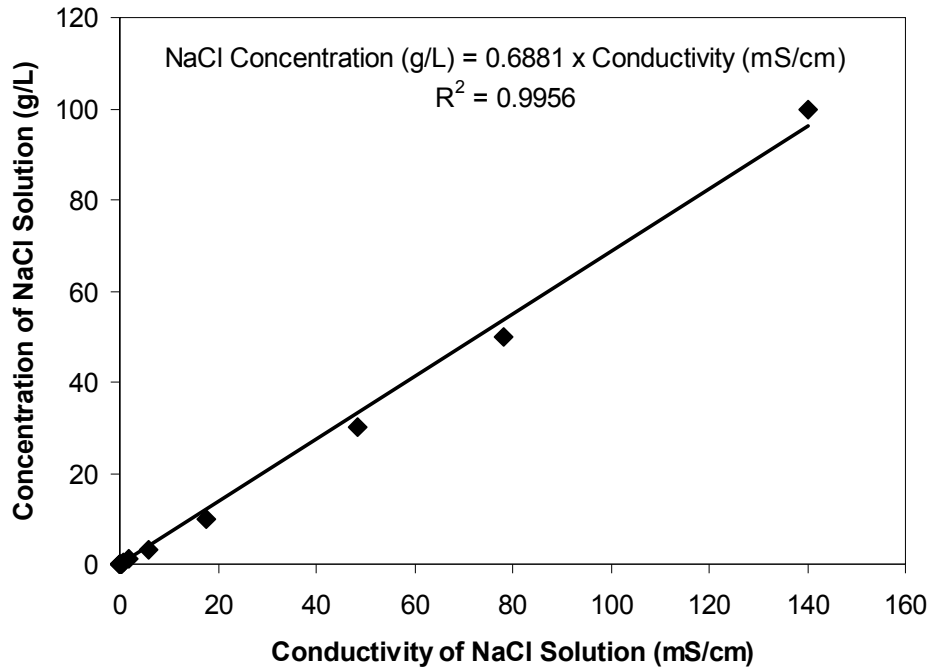
Figure 2.7. Calibration curve of NaCl solution conductivity versus concentration.

From Equation 2-7 and measured conductivity over time, the concentration of salt in the draw solution can be determined, and the osmotic pressure of the draw solution (Π_{feed}) can be calculated by using Equations 2-2 and 2-3. The conductivity of the feed solution (i.e., RO concentrate for most conditions) was also measured over time during the dewater process. For estimation purposes, Equation 2-7 was used to calculate the equivalent "salt" concentration in the feed solution. The osmotic pressure of the feed solution (Π_{feed}) was then calculated by using Equations 2-2 and 2-3. The bulk osmotic driving force $\Delta\Pi$ (or Π_{bulk}) is the difference between Π_{draw} and Π_{feed} (Equation 2-8).

$$\Delta\Pi = \Pi_{draw} - \Pi_{feed} \qquad \text{(Equation 2-8)}$$

Where Π_{draw} = osmotic pressure of the draw solution (psi)
Π_{feed} = osmotic pressure of the feed solution (psi)

At the end of the FO experiment, recovery was calculated by dividing the overall volume of the permeate (calculated from the total weight increase of the draw solution or total weight loss of the feed solution) by the initial volume of feed solution (Equation 2-9).

$$Recovery\ (R) = V_{permeate} / V_{initial\,feed} = \Delta W / (\rho_w\ V_{initial\,feed}) \quad \text{(Equation 2-9)}$$

Where $V_{permeate}$ = volume of the permeate (m^3)
$V_{initial\,feed}$ = volume of the initial feed (m^3)
ΔW = change in weight (kg) through the experiment

ρ_w = density of water (kg/m^3)

The rejection of specific solute by the membrane is calculated by using Equation 2-10.

$$Rejection\ (Rj) = 1 - C_{draw\ solution} / C_{initial\ feed} \qquad \text{(Equation 2-10)}$$

Where $C_{draw\ solution}$ = concentration of solute in the draw solution (mg/L)
$C_{initial\ feed}$ = concentration of solute in the initial feed solution (mg/L)

2.7 ECONOMIC ANALYSIS

A preliminary economic evaluation was conducted for utilizing FO to minimize the volume of RO concentrate produced from a 10-mgd IMS train incorporating MBR and RO. This evaluation compared the cost of integrating the FO concentrate dewatering process into a full-scale IMS facility and comparing this cost with commercially available zero liquid discharge (ZLD) treatment. This economic analysis must be considered preliminary, as the FO process has not been tested at the pilot or full scale on a long-term basis for this particular application. The cost of the FO process was estimated from the bench tests performed for this study.

General assumptions used in the cost estimation follow:

- o Free water recovery of the RO process was considered 80%;
- o RO flux was 12 gfd;
- o Electrical cost was $0.1/ kwh;
- o Interest rate was 5%;
- o Labor cost was $40/h;
- o Plant life was 25 years;
- o All costs were calculated for 2006 dollars;
- o Chemical Engineering Process Cost Indices were used for major process equipment cost escalation;
- o Marshall and Swift Average Annual Equipment Cost Index was used to escalate ancillary membrane equipment costs;
- o Engineering News Record–Construction Cost Index was used to escalate construction costs;
- o Value of the water recovered from the ZLD or FO process was not considered in the analysis.

The two separate treatment train costs estimated as part of the economic analysis are

Train 1 (Baseline Train): MBR/RO/ZLD
This train represents the baseline process for the economic evaluation (Figure 2.8). A ZLD process is used to treat 2 mgd of RO concentrate from a 10-mgd IMS.
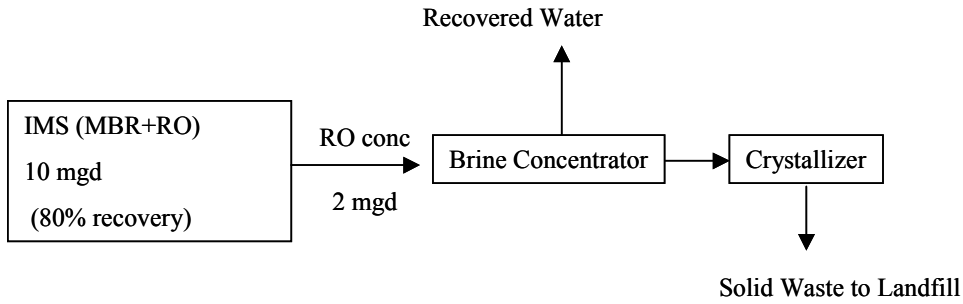
Figure 2.8. A process diagram of the MBR-RO-ZLD system.

Train 2 (FO train): MBR/RO/FO/IX/ZLD

This train represents the use of FO for dewatering 2 mgd of the RO concentrate produced by the RO portion of the IMS train (Figure 2.9).
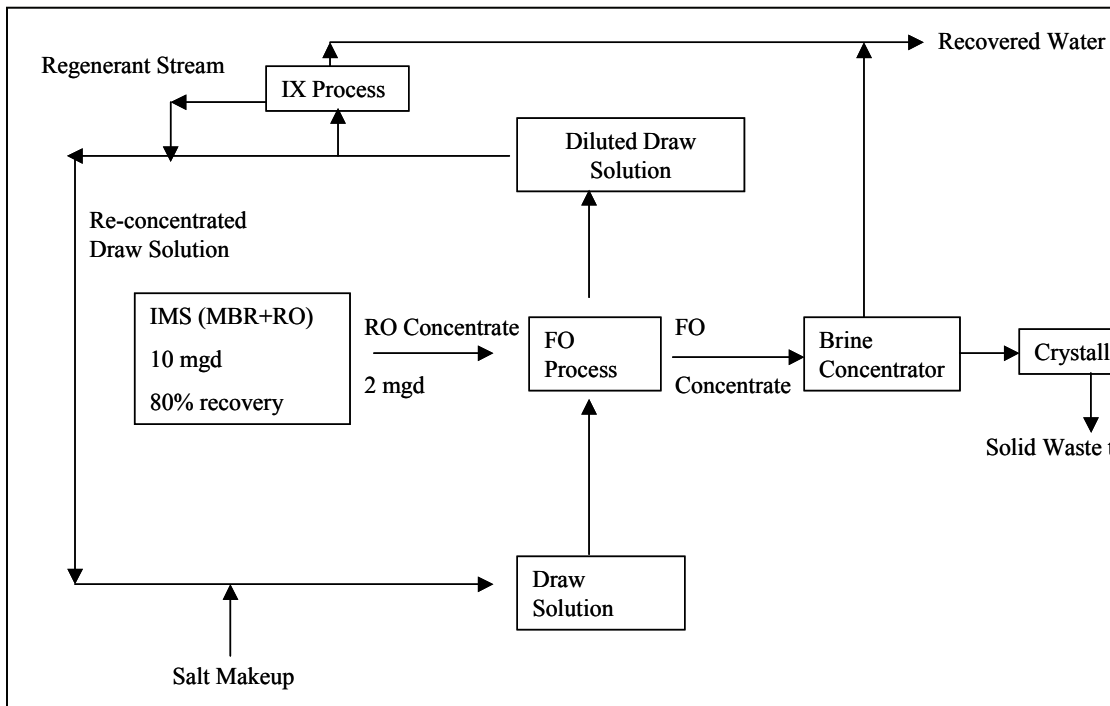
Figure 2.9. A process diagram of the MBR-RO-FO-ZLD system.

CHAPTER 3

RESULTS AND DISCUSSION

This section summarizes the results from the bench-scale testing conducted in this study as well as the results of the economic evaluation.

3.1 CALIBRATION OF DCMO

The design and calibration of a DCMO provided a fundamentally important tool to measure the osmotic pressure provided by innovative draw solutions. Our design of this equipment was necessary because no published methods of measuring any of the colligative properties related to osmolality would provide osmotic pressure data in the range that is applicable to desalination.

All pressure measurements using DCMO represent the gauge pressure relative to atmospheric levels. Upon tightening of the device, the pressure rapidly increased to some tightening pressure in each experiment similar to that experienced by Chahine et al. (2005). Once placed in the bath solution, the pressure increased nonlinearly as a result of water transport across the membrane, reaching equilibrium within 1–10 h. Only equilibrium osmotic pressure results were used in subsequent analyses. Typical pressure response curves for PEG-1500 are shown in Figure 3.1.

The pressure response of PEG-1500 as a function of concentration is shown in Figure 3.2. The measured osmotic pressure data of PEG-1500 has been compared to published data and models reported elsewhere (Cohen and Highsmith, 1997). As shown in Figure 3.2, the diamond symbols and dash lines are regenerated from Cohen and Highsmith's model. The dash lines represent the upper and lower limits of measured osmotic pressure data, while the diamond symbols represent the fitted data. The square symbols present the measured osmotic data by DCMO in our lab. Results show that the direct measurement setup can be used to accurately measure the osmotic pressure of macromolecular and colloidal solutions or suspensions up to 500 psi.
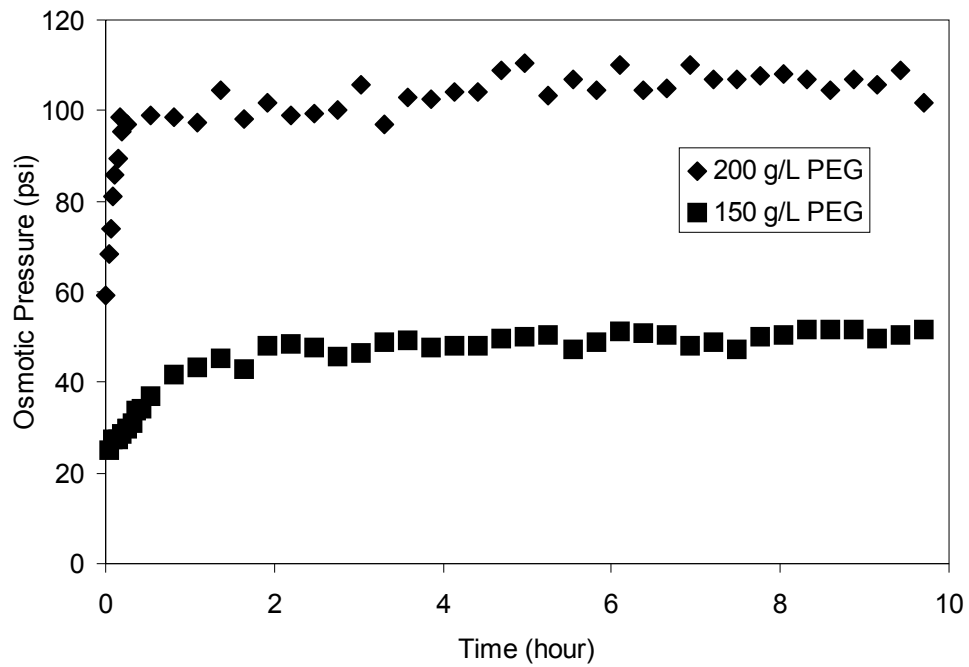
Figure 3.1. Typical pressure responses of DCMO as a function of time.
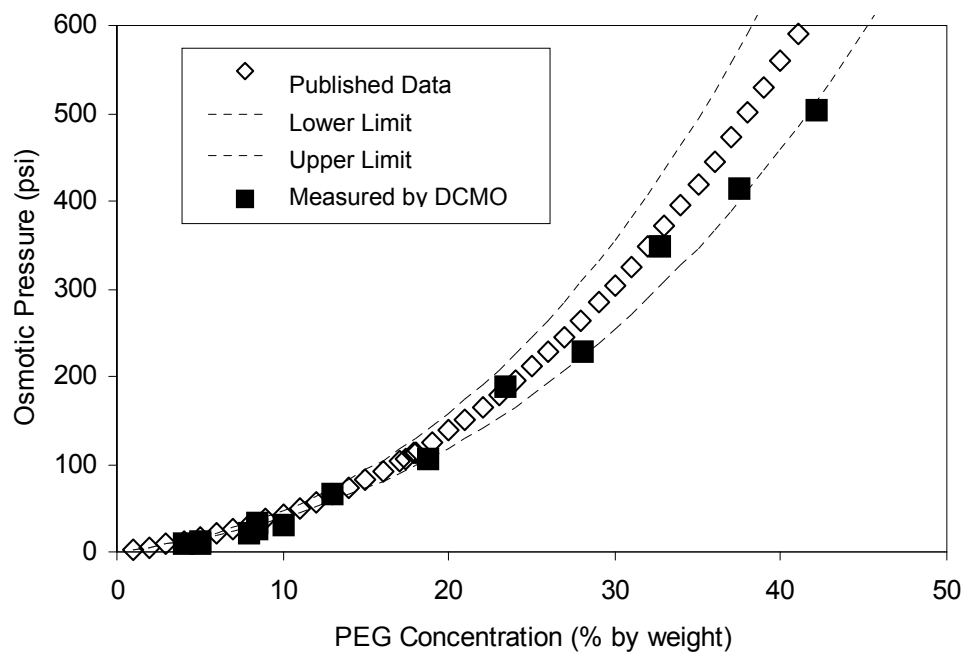
Figure 3.2. Calculated and measured osmotic pressure for PEG-1500.

3.2 EVALUATION OF DRAW SOLUTIONS

3.2.1 Osmotic Pressures Provided by Various Draw Solutions

Sodium Chloride

The osmotic pressure of sodium chloride (NaCl) has been well characterized by researchers (MWH, 2005). As described in Section 2.5.1, the osmotic pressure of sodium chloride solution was calculated by using the modified van't Hoff equation and is presented in Figure 3.3.

Salt (NaCl) has excellent properties as an osmotic agent, including low viscosity and high osmolality. In this study, salt was used as a baseline from which to design and evaluate real-world application of our flow-through system designed for concentrate dewatering by FO.
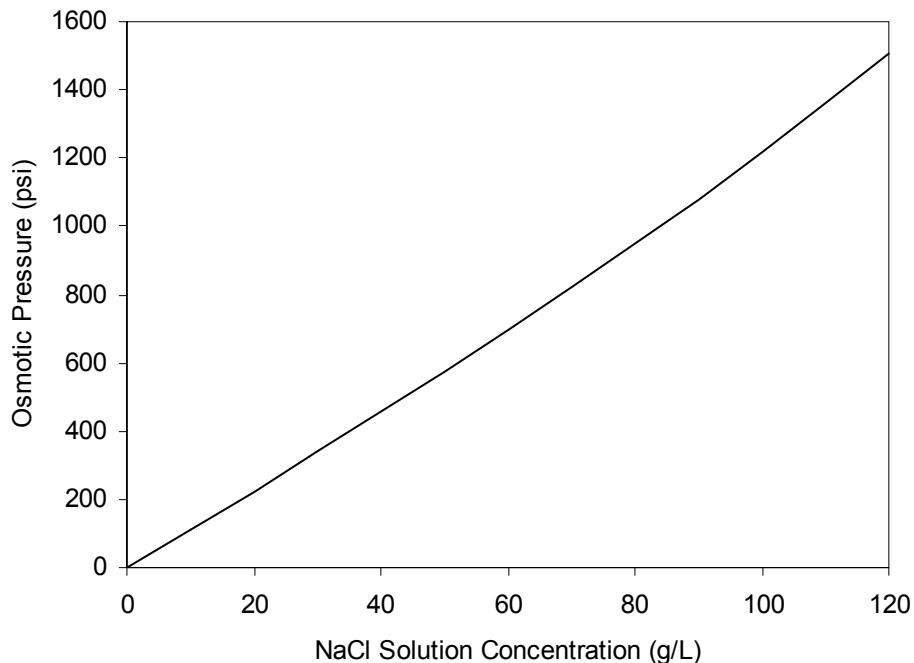
Figure 3.3. Osmotic pressure as a function of solution concentration at 20 ^{o}C for sodium chloride (NaCl) solution.

Magnetic Nanoparticles

Four batches of magnetic nanoparticles were tested by using the DCMO, and the osmotic pressure results are provided in Table 3.1. The highest osmotic pressure result was 25 psi for the 45% (w/w) PEG-gylated sample with surface charges contributed by quaternary ammonium groups. The addition of surface charge to the nanoparticles increased the osmotic pressure, as sample 2 with extra quaternary ammonium groups demonstrated a slightly higher osmotic pressure than did sample 3, even though the concentration of the latter was higher.

Table 3.1. Osmotic Pressure Characterization of Magnetic Nanoparticles

Sample No.	Weight Percent (%)	PEG Coated	Quaternary Ammonium Group Attached	Calculated[a] Osmotic Pressure (psi)	Measured Osmotic Pressure (psi)
Sample 1	25	No	No	0.6	3
Sample 2	27	No	Yes	0.7	6.6
Sample 3	37	No	Yes, but less charge per particle than in sample 2	1.1	5.5
Sample 4	45	Yes	Yes, reacted with an excess of quaternary ammonium	1.5	25

[a]Calculated by using Equation 2-1, assuming no multiple ionizable solutes, no charge on the nanoparticles, osmotic coefficient = 1.

The low osmotic pressure associated with the magnetic particles can be explained by the high molecular weight and low solubility of the solute. The nanoparticles might also not be very attractive because of their unfavorable physical properties. As shown in Figure 3.4, the magnetic fluid tested was highly hydrophobic and viscous.
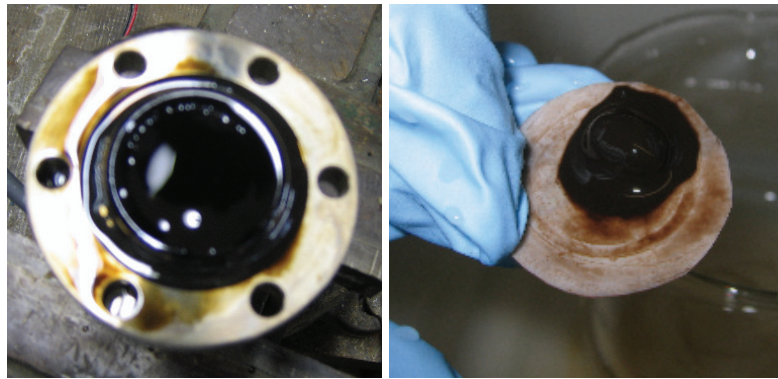
Figure 3.4. Photograph of magnetic nanoparticles.

Our measurements, however, have shown that magnetic nanoparticles may have potential if they can be appropriately synthesized. At the low volume percentages (14 %) measured, the pressures were still significant (25 psi). If the nanoparticles can be designed to be smaller and less viscous with a greater hydrophilic surface, then higher osmotic pressures may be obtainable. For example, we observed that the PEG-coated magnetic nanoparticles had a significantly higher osmotic pressure than did the uncoated nanoparticles of similar concentration (Table 3.1). These coated particles were more hydrophilic, and the magnetic fluid was less viscous. Additional research is needed to further explore the potential of custom-designed nanoparticles that might yield the desired properties.

Rapid-throughput methods of magnetic separation of magnetic nanoparticles have been utilized in biomedical and biological research (Pankhurst et al., 2003). It has been reported that coated magnetic nanoparticles can be captured by high-gradient magnetic separation systems with a canister separator (Moeser et al., 2004). The magnetic nature of the nanoparticles will facilitate the removal of solute, which meets one of the important criteria for the ideal draw solution.

Albumin

BSA has been tested as the draw solution and the osmotic pressure results are shown in Table 3.2. These measured data correlate with the literature (Scatchard et al., 1944). The highest osmotic pressure measured was 7 psi for 30% (w/w) BSA solution. As BSA has a high molecular weight (around 66,000 g/mol), the osmotic pressure provided by this compound is not sufficient for use as a draw solution. Upon heating, the albumin solution was denatured and solidified. Water could be separated from the solidified albumin, but the recovery is low.

Table 3.2. Osmotic Pressure Characterization of Albumin Solutions

Sample ID	Weight Percent (%)	Calculated[a] Osmotic Pressure (psi)	Measured Osmotic Pressure (psi)
Sample 1	15	1	4
Sample 2	30	3	7

[a] Calculated by using Equation 2-1, assuming that the albumin is iso-ionic, osmotic coefficient = 1.

Dendrimer

A dendrimer is a synthetic macromolecule with a self-similar fractal branching geometry. It has the unique ability to contain a maximized number of terminal functional groups (Tomalia et al., 1985). With appropriate functional groups on the surface, the dendrimer molecule can be highly charged. The particles are very small and can provide high osmotic pressure, especially when the surface functional groups are dissociated at the proper pH, thus supplying a large number of ions contributing to the osmotic pressure.

Table 3.3 presents the osmotic pressures of dendrimers measured by the DCMO at ambient pH. If the sodium ions on the dendrimer surface did not dissociate in the solution, the osmotic pressure would be significantly lower than the measured values. For example, calculations using the van't Hoff equation show that 5% (w/w) of G2-EDA dendrimer (sample 1) may provide only 3.4 psi if calculated from the molar concentration of the dendrimer alone but may result in 17-fold-higher (58 psi) pressure if all 16 surface sodium ions dissociate from the terminal–COONa groups present on the dendrimer surface. The measured osmotic pressure was 34 psi, between the two values, indicating that the surface sodium ions were partially dissociated. For dendrimers of higher generations (G3 and G5, samples 2 and 3 respectively), the measured osmotic pressures were lower. It is hypothesized that the dissociation of surface ions per particle is lower as the generation increases at ambient pH, probably because the charges are too close together at higher generations.

Table 3.3. Different Types of Dendrimers and Their Osmotic Pressures

Sample ID	Core	Mol Wt (Da)	Terminal Group Attached	Weight Percent (%)	Expected[a] Pressure (psi) Not Dissociated	Fully Dissociated	Measured Osmotic Pressure (psi)
1	G2-EDA	5204	16 of sodium succinamate	5	3.4	58	34
2	G3-EDA	10,804	32 of sodium succinamate	5	1.7	54	29
3	G5-EDA	44,404	128 of sodium succinamate	5	0.4	51	14
4	G2-pentaearythirityl	4027	24 of sodium carboxylate	20	17.8	438	330

[a]Calculated by using the van't Hoff equation (Equation 2-1).

Dendrimers might be a promising osmotic medium, as these macromolecules can be synthesized to provide high osmotic pressure. As shown in Table 3.3, sample 4, a 20% (w/w) solution of G2-pentaearythirityl sodium carboxylate dendrimer was measured at 330 psi (ambient pH). The dissociation of surface sodium ions contributes a large fraction of this osmotic pressure. Since the chain length of the carboxylate group is half that of a succinamate group, the number of surface groups per volume was much higher for the carboxylate dendrimer (sample 4) than for the other three succinamate dendrimer samples. This might contribute to the high osmotic pressure measured for sample 4.

3.2.2   Reconcentrate Strategies for Promising Draw Solutions

Sodium chloride and dendrimers were selected as the most promising draw solutions as they are able to provide the highest osmotic pressures. For these two solutions, the removal mechanisms and reconcentration strategies were further studied at a proof-of-concept level.

Sodium Chloride

Sodium chloride solution is relatively simple to reconcentrate by using proven desalting methods. The combination of FO and RO has been used to treat leachate (Osmotek, 2003), and the diluted draw solutions (NaCl) were reconcentrated with RO without risk of scaling. Also conceptually, the pure sodium chloride solution (without any divalent ions or other impurities) can be reconcentrated by using electrodialysis (ED) or ion exchange (IX). As shown in Figure 3.5, a suitable process could be added to reconcentrate the draw solution after it has been diluted in the FO process.
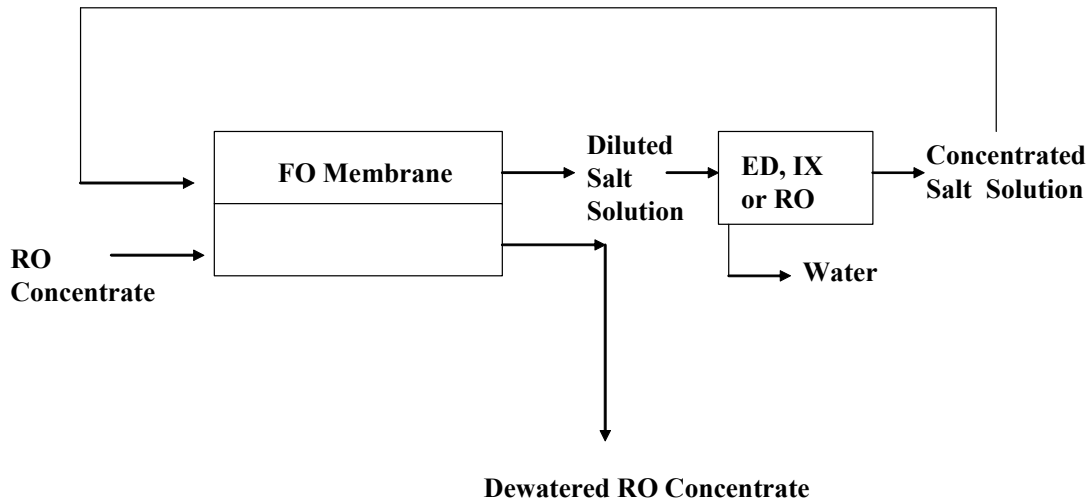
Figure 3.5. Schematic of salt reconcentrating system using ED, IX or RO.

Dendrimers

The reconcentration of dendrimer was also explored at the proof-of-concept level. The dissociation of the surface groups on the dendrimer is likely to be controlled by the pH (Diallo et al., 2005). When the pH is lower than the pKa of the dendrimer, the surface sodium ions may dissociate from the dendrimer and contribute to high osmotic pressure. For reconcentration of the dendrimer draw solutions, the pH can be adjusted so that the sodium ions would rebind to the dendrimer surface and be removed along with the dendrimer body by a UF process. Removal of metal dendrimer complexes by UF has been reported by others (Diallo et al., 2005). The schematic for this reconcentration process is shown in Figure 3.6.
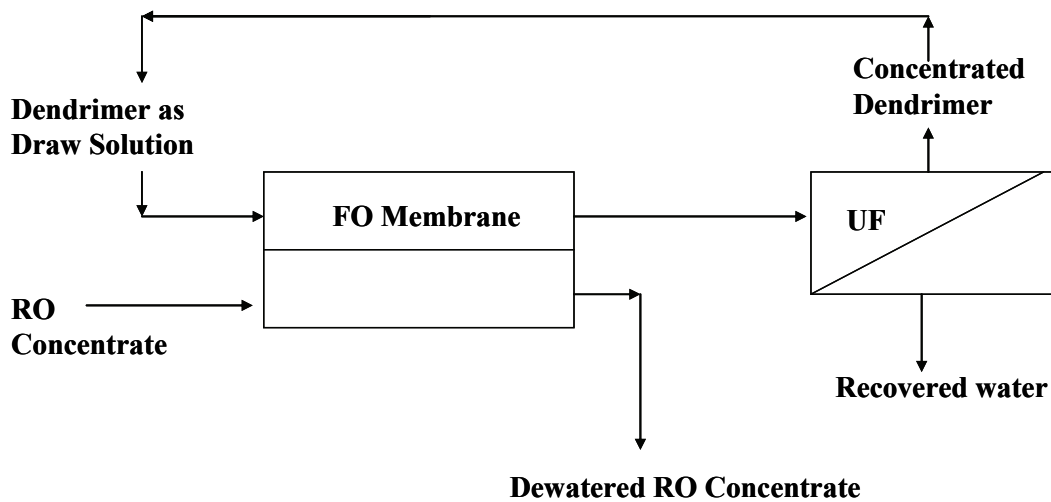
Figure 3.6. Schematic of dendrimer reconcentration process.

To investigate the pH dependence of the dissociation of the surface functional groups, the project team attempted to measure the osmotic pressure of 20% G2-pentaearythirityl sodium carboxylate dendrimer (sample 4 in Table 3.3) over a wide pH range. The experiment, however, encountered the difficult need for a large amount of acid or base to adjust the pH of tested dendrimer. For example, to adjust the dendrimer solution from ambient pH 9.52 to pH 2.96, 0.58-mol/L HCl solution was added. The addition of this excess amount of acid introduced extra ions to the solution, which interfered with the osmotic pressure measurement of the dendrimer solution. Further study should be conducted with dendrimers of low buffering capacity to explore the pH-dependent dissociation of surface ions and osmotic pressure.

As an alternative, a direct UF experiment was conducted at ambient pH with G2-pentaearythirityl sodium carboxylate dendrimer to test the recovery of this material. One hundred milliliters of 2% dendrimer solution (ambient pH of 10.66) was filtered through an UF membrane (molecular weight cutoff [MWCO] of 1000) in an Amicon stirred cell (model 8200; Millipore), resulting in 50 mL of concentrated dendrimer (pH = 10.55) and 48 mL of filtrate (pH = 10.86). The molecular weight of this dendrimer is 4027 g/mol, including 24 surface sodium ions. Excluding the sodium ions, the organic "body" of the dendrimer has a molecular weight of 3475 g/mol. If the surface sodium ions were fully dissociated during the UF, we would have observed a high concentration of sodium in the filtrate stream, as the 1000-MWCO UF membrane would reject the large dendrimer "body" but not the small dissociated sodium ions.

Table 3.4 shows the sodium concentrations in the concentrate and in the filtrate. Surprisingly, the sodium concentration measured in the filtrate was significantly lower than in the concentrate. The UF membrane rejected 87.3% of the sodium in the dendrimer solution, although the pores of the membrane were much larger than were the sodium molecules. The sodium may be associating with the dendrimers during UF because of the necessity of maintaining electroneutrality in both the filtrate and the retentate.

Table 3.4. UF Test on 2% of G2-Dendrimer Solution

2% Dendrimer Condition	Vol (mL)	pH	Sodium (mg/L)
Before filtration	100	10.66	2600
Concentrate	50	10.55	4500
Filtrate	48	10.86	570

UF has the potential of recovering the dendrimer together with the surface ions, as demonstrated in this study. The reconcentrated material could be used as the osmotic medium to provide high osmotic pressure in the FO process. The rejection of small surface ions by UF might be enhanced if the surface of the UF membrane is modified with the same type of charge as for the surface ions or if the pH of the dendrimer solution is controlled to ensure the minimum discharge of surface ions.

Further studies may be conducted to explore the pH-controlled UF of dendrimers that have ionizable surface ions (like sodium) and low buffering capacity. Specially designed dendrimers with these properties could be easily adjusted to a wide range of pH conditions without introducing an excessive amount of the pH-adjusting ions. The samples with adjusted pH could be ultrafiltered, and the concentration of surface ions in the filtrate could be minimized to enhance the recovery of the surface ions in the reconcentrated dendrimer solution.

3.3 EVALUATION OF MEMBRANES

Four flat-sheet and one hollow-fiber membranes were obtained from different manufacturers for this project. The hollow-fiber membrane E came in wet as a whole RO module, and it was very difficult to convert it to a flow-through FO system. Membrane A, a flat-sheet brackish RO membrane, was tested with the osmometer (see Section 2.5.2) and proved to be too thick to use (the time taken to reach equilibrium was too long). The other three flat-sheet membranes (B, C, and D) were characterized in terms of permeability and salt rejection in flow-through RO and FO systems (Section 2.4.2), and the results are summarized in Table 3.5.

Table 3.5. Osmotic Permeability and Salt Rejection of Three Flat-Sheet Membranes (B, C and D)

Membrane Used	Specific Flux in RO Mode (gfd/psi)	Flux and Salt Rejection in RO Mode (%)		Specific Flux in FO Mode (gfd/psi)	Flux and Salt Rejection in FO Mode (%)	
		Flux (gfd)	Rejection (%)		Flux (gfd)	Rejection (%)
Membrane B	0.0368	2.3	85.8	0.0172	5.2	99.3
		3.4	86.1		8.2	98.9
		5.1	89.9			
		6.6	91.3			
		9.3	89.9			
Membrane C	0.0244	1.8	89.6	0.0115	3.8	99.9
		3.1	91.8		6.1	99.9
		4.0	94.1			
		5.6	95.7			
		6.1	95.9			
Membrane D	0.185	4.6	95.6	0.00241	0.6	99.9
		14.1	96.7		0.9	99.9
		24.7	98.3			
		34.9	98.0			
		47.8	98.0			

Membranes B, C, and D were first operated in a cross-flow RO mode. Membrane D showed the highest permeability, with a specific flux of 0.185 gfd/psi. The permeability of membranes B and C is much lower than that of membrane D under RO mode. The specific flux of these two membranes is less than 20% that of membrane D. The salt rejection was generally better when the water flux was higher. Membrane B showed lower salt rejection than did the other two membranes.

When tested under the FO mode, membranes B and C had significant higher permeability than did membrane D. As membrane B demonstrated the greatest osmotic permeability in the FO mode (specific flux of 0.0172 gfd/psi), it was identified as the best membrane and used in subsequent experiments. All three membranes showed high salt rejections (greater than 98%), as there was only a trace amount of salt diffusing through the membrane. It is important that the rejection reported in the permeability test was possibly higher than the actual rejection that would occur during the dewatering of RO concentrate. The rejection measured during the FO permeability test resulted from the diffusion of salt across the membrane, since the salt passage across the membrane was in the reverse direction of the water. When RO concentrate, in contrast, is being dewatered, the salt in the RO concentrate passes through the membrane to the draw solution side in the same direction as the water does, and the rejection of FO designed to dewater RO concentrate results mostly from the convection of salt across the membrane with water. As more salt will be carried across the membrane with water, this convection might yield lower rejection values than does the diffusion in the permeability test.

3.4 CROSS-FLOW FO EXPERIMENTS

FO cross-flow tests were conducted with NaCl draw solutions and deionized water or RO concentrate as feed solutions. The impact of membrane type, draw solution concentration, in-line UF, pretreatment of feed water, and membrane cleaning on the process performance was investigated. Additionally, an FO cartridge was tested to explore the utility of this dewatering process. The results are presented below.

3.4.1 Tests with Deionized Water

Effect of Membrane Type on Water Flux

As discussed in Section 3.2, the different membranes tested demonstrated different osmotic permeability in the flow-through FO tests. Figure 3.7 shows the changes in the water flux as a function of osmotic pressure difference for three types of membranes tested under similar conditions (feed: deionized water; draw: 45-g/L NaCl; draw solution facing the active layer). For each experiment, as water passed across the membrane, the draw solution was diluted and the osmotic pressure difference decreased. The water flux dropped with decreasing osmotic pressure differences from the initial highest value. This figure shows the water flux achieved by membrane B was higher than by membranes C and D at the same osmotic pressure difference. The maximum flux achieved was 10.4 gfd by membrane B at the beginning of the run.
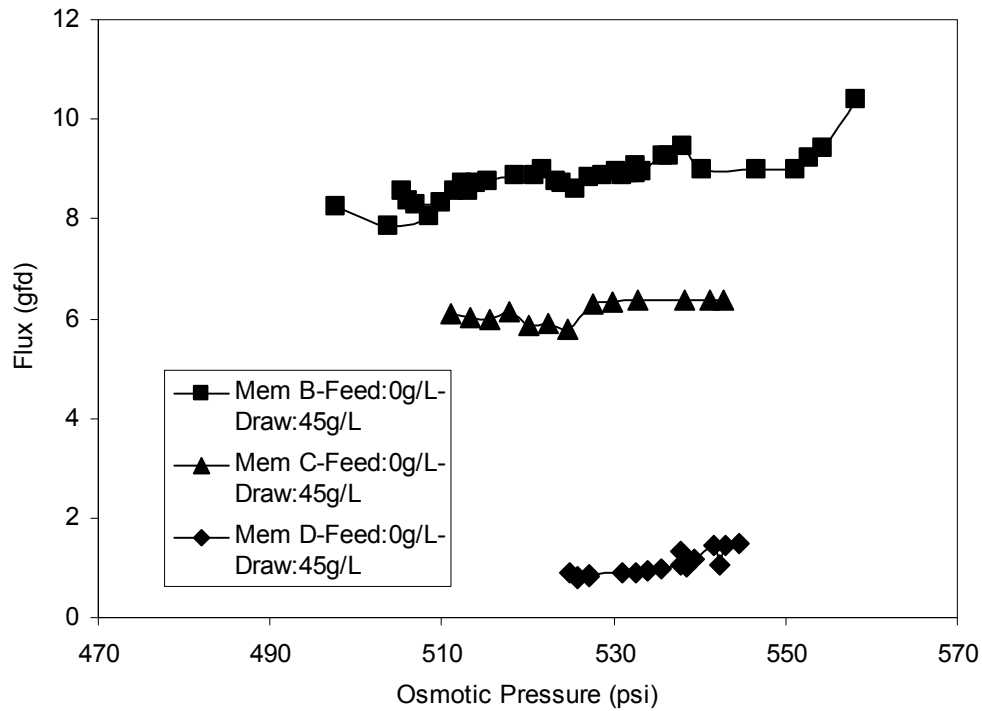
Figure 3.7. Comparison of water flux of three membranes with deionized water as the feed solution.

Figure 3.8 shows the changes in specific flux as a function of osmotic pressure when the membranes were operated under the conditions mentioned above (feed: deionized water; draw: 45 g/L NaCl; draw solution facing the active layer). The specific flux indicated the osmotic permeability of the membrane and was mostly constant through operation. As shown in this figure, membrane B has the highest osmotic permeability and the water flux obtained from using this membrane at the same osmotic pressure difference will be the greatest compared to those obtained by using the other two membranes.
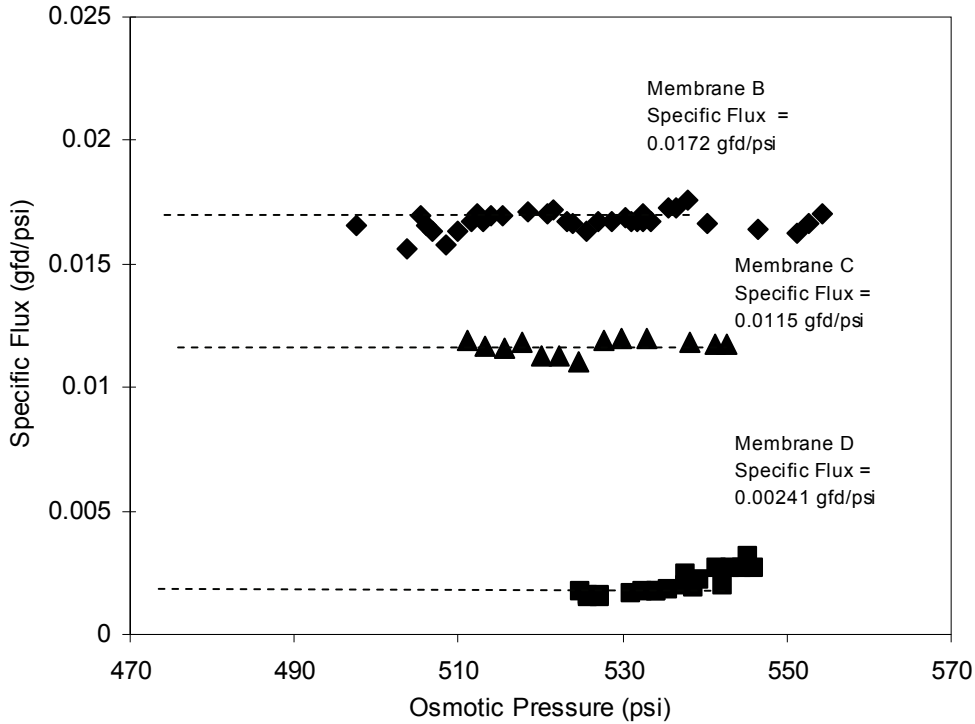
Figure 3.8. Comparison of specific flux of three membranes with deionized water as the feed solution.

Effect of Draw Solution Concentration

The osmotic permeability tests with deionized water as the feed were also conducted with different concentrations of NaCl as the draw solution. Figure 3.9 shows that the water flux changes are almost linear with the osmotic pressure difference. When membrane B was facing 30-g/L NaCl solution on the active layer side, 6 gfd of flux was obtained. Compared with results obtained by McCutcheon et al. (2005), the results in this study are significantly different. They reported 19 gfd of flux for 0.5 M (29 g/L) NaCl as the draw solution on the active layer and deionized water on the support layer at 50 °C and cross-flow velocity of 21.4 cm/s. This substantial difference in flux can be attributed to the difference in membrane and experimental conditions. In this study, all FO experiments were conducted at room temperature (22 °C) and cross-flow velocity of 15.4 cm/s. The decrease of temperature and cross-flow velocity in this study could result in decreased water flux produced by FO.
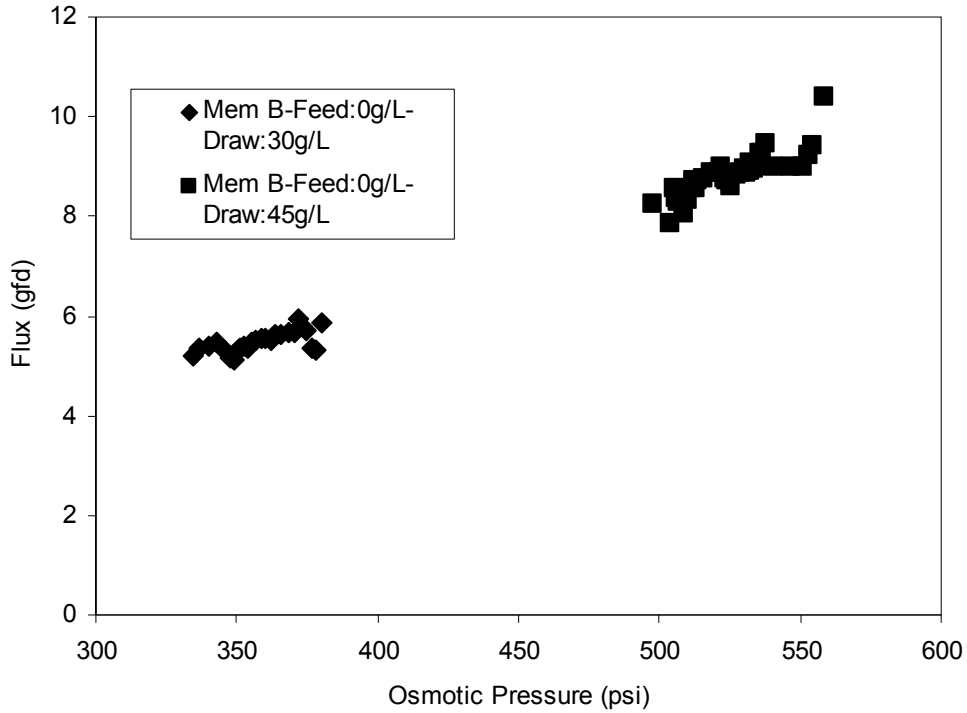
Figure 3.9. Water flux at different concentrations of draw solution with deionized water as the feed solution.

If we normalize their data to 22 °C by using Equation 3-1 to account for the variation of water viscosity with temperature, 19 gfd at 50 °C is equivalent to 9.7 gfd at 22 °C, which is higher than the 6 gfd observed in this study at 22 °C. The difference in flux might be attributed to varied cross-flow velocity (21.4 cm/s versus 15.4 cm/s) and membrane difference. Moreover, the increase in temperature might help with creating better flow conditions and minimizing the CP besides reducing the viscosity, and this effect was not totally accounted for by Equation 3-1.

$$J \ (at \ 22 \text{°C}) = J \ (at \ 50 \text{°C}) \times 1.03^{(22 - 50)} \qquad \text{(Equation 3-1)}$$

When the same piece of membrane was operated with different concentrations of draw solutions, the specific flux was almost the same (Figure 3.10).

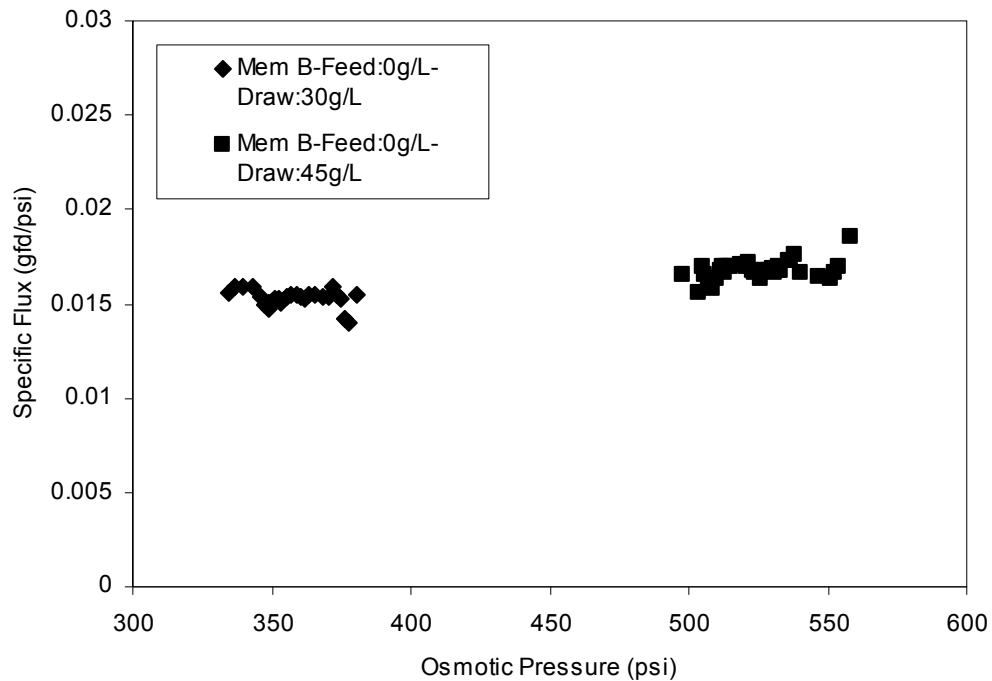**Figure 3.10. Specific flux at different concentrations of draw solution with deionized water as the feed solution.**

The specific flux was controlled by the intrinsic permeability of the membrane and CP. In this case, as shown in Figure 3.11, as deionized water faced the porous support layer, the effect of concentrative internal CP in the support layer was minimal since the salt concentration in the deionized feed was very low. The dilutive external concentration polarization occurring on the permeate side (the active layer) might have a greater impact. The concentration of the draw solution at the membrane surface would be lower than in the bulk, as water permeates the membrane from the feedwater side. The calculated specific flux might underestimate the membrane permeability since the actual driving force (i.e., effective osmotic pressure difference $\Delta\Pi_{eff}$) would be smaller than the bulk osmotic pressure difference $\Delta\Pi_{bulk}$ because of dilutive external CP. It was expected that the external CP was greater when the draw solution had a higher concentration, since the water flux would be greater. Therefore, the apparent specific flux would be decreased with increased draw solution concentration (McCutcheon et al., 2005). However, in this part of the study, we didn't observe a significant external CP effect, as the specific flux was mostly unchanged with increased draw solution concentration. Possible explanations could include the small variation (30 g/L versus 45 g/L) in draw solution concentrations or mitigated external CP under the experimental conditions.
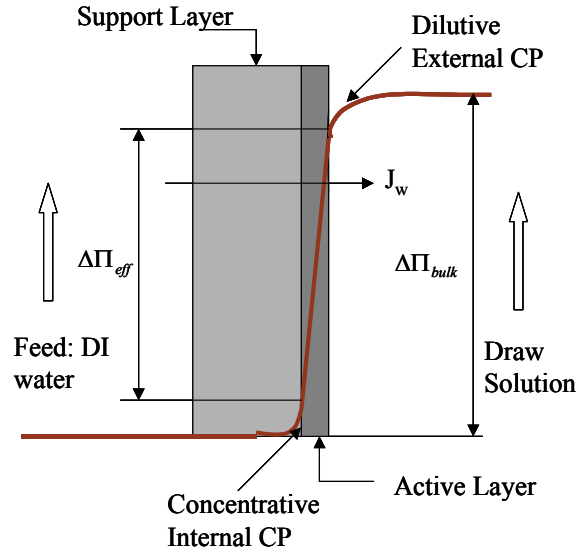
Figure 3.11. Schematic of CP with deionized water as the feed solution.

3.4.2 Tests with RO Concentrate

The water quality of the RO concentrate collected from the IMS pilot at Rio Rancho, NM, is provided in Table 3.6. The osmotic pressure of the RO concentrate was calculated as 27 psi by using Equation 2-1 and taking into account all of the major ions.

Table 3.6. Water Quality of the RO Concentrate

Parameter	Unit	RO Concentrate
Calcium	mg/L	110
Magnesium	mg/L	11
Barium	μg/L	95
Potassium	mg/L	100
Iron	mg/L	0.11
Silica	mg/L	100
Sodium	mg/L	690
Manganese	μg/L	34
Strontium	mg/L	2
Boron	mg/L	1.4
Phosphate	mg/L as P	10
Sulfate	mg/L	492
Nitrate	mg/L	194
Chloride	mg/L	804
TDS	mg/L	2950
Hardness	mg/L as $CaCO_3$	295
Alkalinity	mg/L as $CaCO_3$	520
Conductivity	mS/cm	3.6

Effect of Draw Solution Concentration

Two liters of RO concentrate was dewatered in each FO run by using the flat-sheet membrane B. Initially, FO experiments were conducted to test the choice of using 1 L of 100-g/L NaCl or 2 L of 50-g/L NaCl as the draw solution. As shown in Figure 3.12, the initial specific flux was 0.0134 gfd/psi when 2 L of 50 g/L NaCl was used as the draw solution. After 900 min of operation, the specific flux was reduced to 0.005 gfd/psi and the final recovery was 60%. The initial specific flux was slightly lower (0.0109 gfd/psi) when 1 L of 100-g/L NaCl was used as the draw solution. After 1200 min of operation, the specific flux dropped to 0.003 gfd/psi and the final recovery was 71%. It is economically favorable to use 1 L of 100-g/L NaCl instead of 2 L of 50-g/L NaCl as the draw solution, since a smaller volume of diluted draw solution will be generated at the same feed recovery.
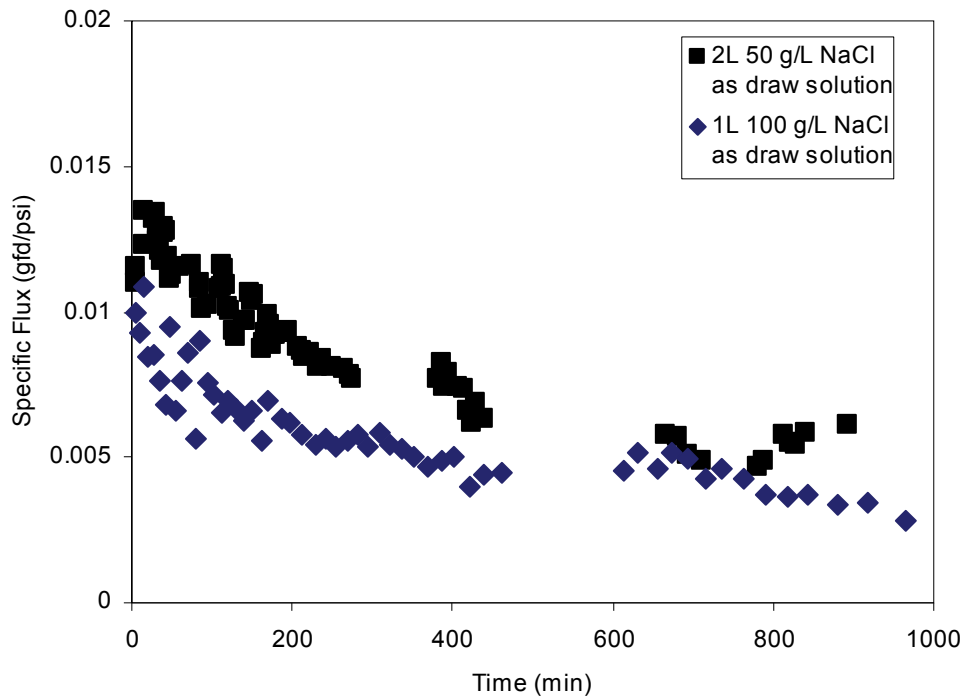
Figure 3.12. Impact of draw solution concentration on the FO specific flux with RO concentrate as the feed solution.

For both draw solutions, the initial specific flux was significantly lower than the clean water specific flux (0.0172 gfd/psi, Section 3.3.1). The decrease might be caused by the concentrative internal CP on the support layer side as shown in Figure 3.13. Upon contact with the support layer, the feed (RO concentrate) diffuses into the porous support layer. As water permeates the activated layer, the feed solution in the support layer is further concentrated, and the feed concentration at the active layer is higher than in the bulk, and this reduces the driving force. The water flux is higher at a higher NaCl concentration (100 g/L in this case), and the internal CP becomes more obvious. Thus, the specific flux for the 100-g/L NaCl solution was slightly lower than that for the 50-g/L NaCl solution.
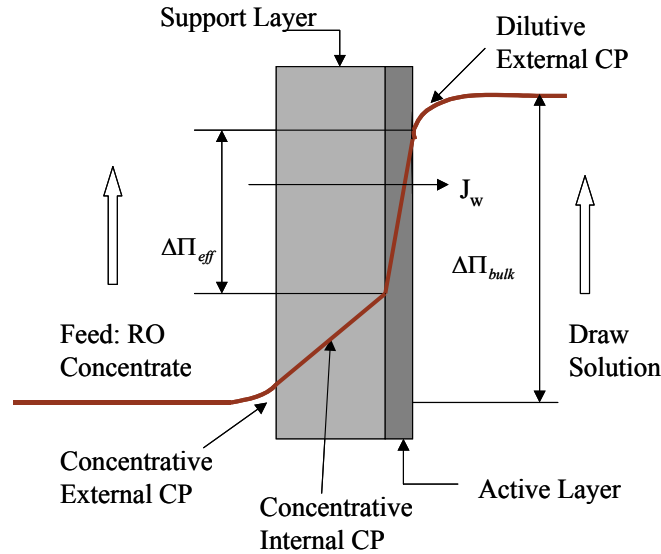
Figure 3.13. Schematic of CP with RO concentrate as the feed solution.

Figure 3.14 shows the decrease of normalized specific flux over time caused by membrane fouling and/or scaling. The two FO experiments with different draw solutions showed similar fouling trends. After 800 min, the specific flux reduced to 40% of the initial water flux. The comparison of normalized specific flux helped to minimize the impact of initial specific flux, thus ensuring the appropriate comparison between two membranes.

Figure 3.14. Impact of draw solution concentration on the normalized FO specific flux with RO concentrate as the feed solution.

When the 1 L of 100-g/L NaCl was used as the draw solution, the final recovery was 71% after 1200 min of operation. At the end of the experiment, the dewatered RO concentrate and diluted draw solution were analyzed for the major elements and rejection of specific ions were calculated. As shown in Table 3.7, a rejectio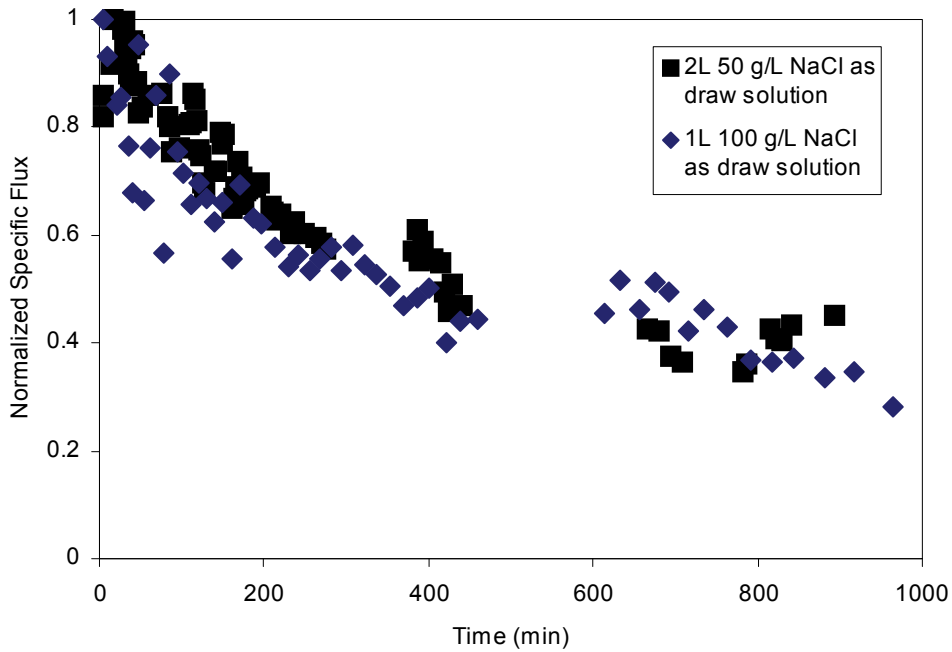n of above 90% was achieved for the major ions except for boron. The decrease of calcium and silica concentrations in dewatered RO concentrate might be caused by the sink in the solid precipitates.

Table 3.7. Water Quality of Dewatered RO Concentrate and Diluted Draw Solution

Parameter	Unit	RO Concentrate	Draw Solution	Rejection (%)
Calcium	mg/L	110	6.4	94.2
Magnesium	mg/L	11	0.55	95.0
Silica	mg/L	100	8	92.0
Sodium	mg/L	690	21,000	NA
Strontium	mg/L	2	0.17	91.5
Boron	mg/L	1.4	0.74	47.1

At the end of the experiment, the membrane cell was opened, and the precipitate on the membrane surface was collected. Professional Water Technologies analyzed the morphology and composition of this precipitate by using SEM and T-EDXA. Figure 3.15 shows the morphology of the precipitate under SEM. The precipitate material was "fluffy" with a wide range of size distribution. The size of precipitated particles ranged from 5 μm to less than 1 μm. The T-EDXA analysis indicated that the precipitate was mostly calcium (99.3%) with a little silica (0.7%).

The analysis indicated that the scaling was essentially $CaCO_3$. Calcium carbonate scales that form slowly over time usually have a variety of coprecipitants apparent in the analysis because of the tendency of a variety of scales to form on calcium carbonate seed crystals present in the feed. The absence of the coprecipitates in our study indicates that the scale formation likely occurred due to a single episode.
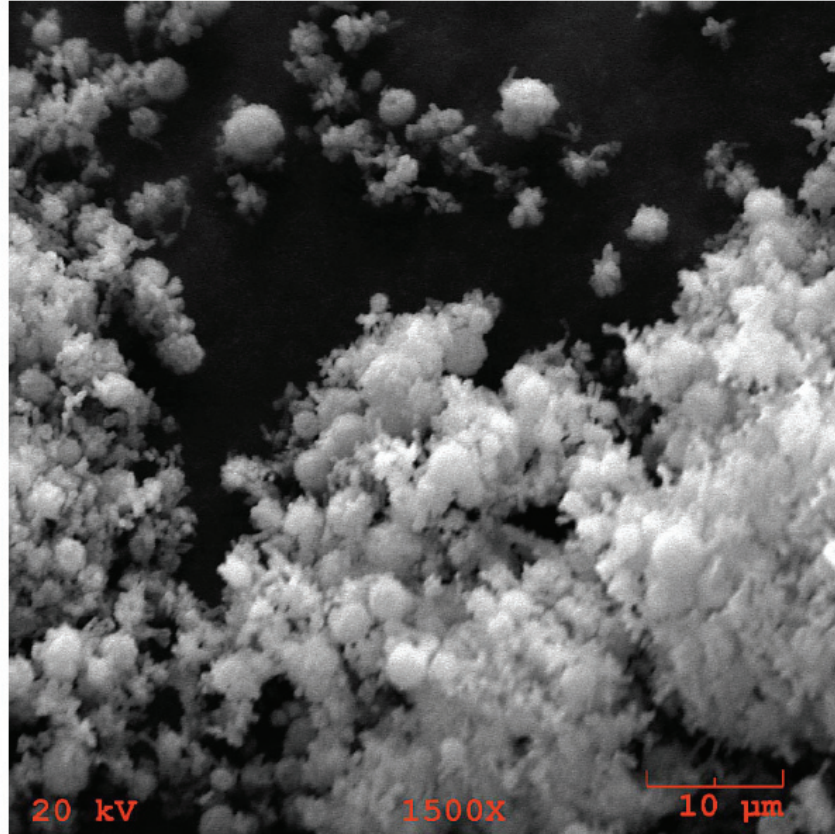
Figure 3.15. SEM image of the FO precipitates.

Effect of Feed Softening

The feed RO concentrate was softened with 300 mg of dolomitic lime/L and 100 mg of ferric chloride/L at initial pH of 11. The research team had previously observed (MWH, 2006) that this softening condition removed a maximal amount of hardness-causing elements and silica in this RO concentrate (Table 3.8).

Table 3.8. Efficiency of Softening Procedure in Removing Hardness and Silica

Parameter	Unit	RO Concentrate	Softened RO Concentrate	Percent Removed (%)
Hardness	mg/L as $CaCO_3$	295	49	83
Silica	mg/L	100	62	38
Conductivity	mS/cm	3.6	5.6	Increased

Figure 3.16 shows that softening the RO concentrate can recover the decreased specific flux. The specific flux without feed pretreatment decreased to 52% of the initial value after 600 min of operation, while the specific flux fell to 60% of the initial flux with the softened RO concentrate. The specific flux was higher by 8% after 600 min when feed softening was used. More optimization is needed in future research.
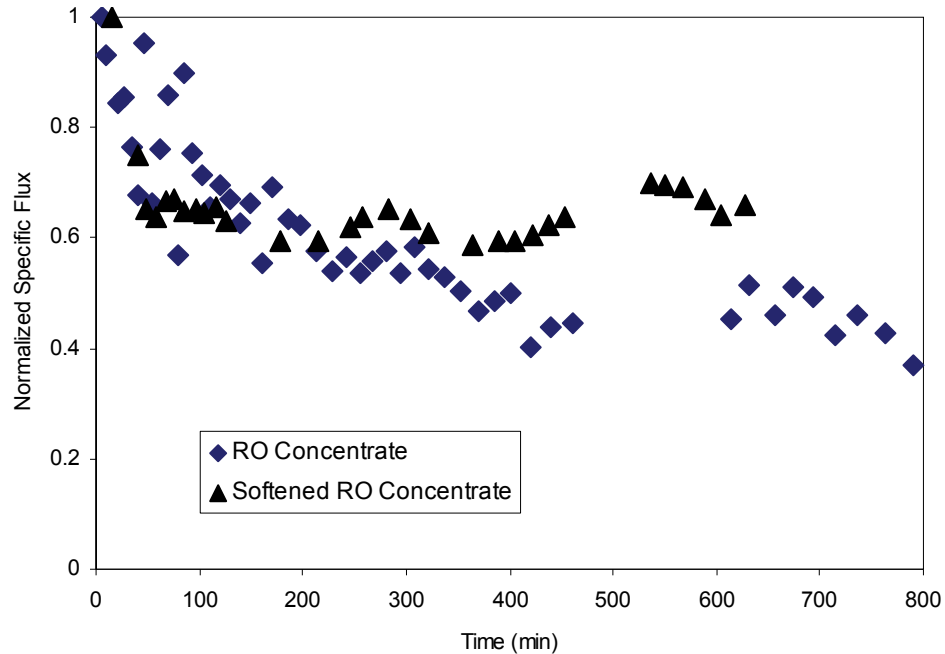
Figure 3.16. Impact of feed softening on the normalized FO specific flux with RO concentrate as the feed solution.

Effect of Membrane Cleaning

Figure 3.17 shows that the specific flux decreased to 23% of the original specific flux after 22 h of operation. The fouled FO membrane was cleaned by 2% of citric acid, and the specific flux was recovered to 81% of the initial specific flux. It is important that the membrane used in this experiment was cleaned ex situ. The elements should be cleaned in situ through several low-pH washes if the flow channels are heavily obstructed. This action might further enhance the chemical cleaning efficiency.
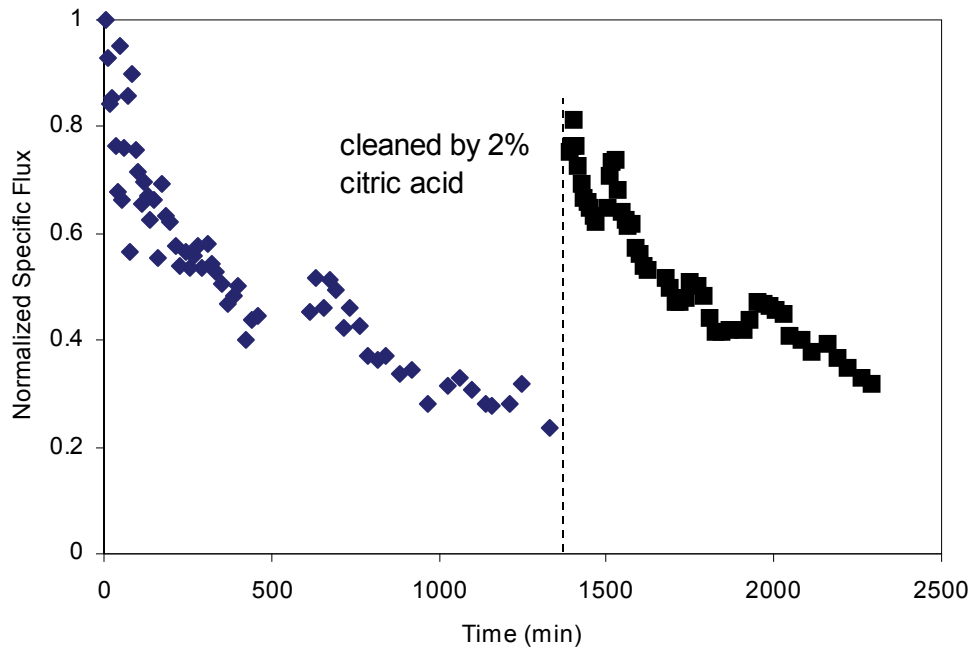
Figure 3.17. Impact of membrane cleaning on the normalized FO specific flux with RO concentrate as the feed solution.

Dewatering RO Concentrate by Using Spiral-Wound FO Membrane

The FO testing with a spiral-wound cartridge was conducted to explore the possibility of expanding the bench testing to pilot scale to treat a large volume of RO concentrate. Eight liters of RO concentrate was dewatered by 2 L of 100-g/L NaCl solution at a flow rate of 0.17 L/min (equivalent to 2.6 cm/s of cross-flow velocity). The total membrane area contained in the FO cartridge was 1.5 m^2. The experiment lasted about 5.8 h as the draw solution was quickly diluted and flux was significantly dropped. As shown in Figure 3.18, the specific flux decreased to 0.001 gfd/psi after 300 min of operation, which was about 34% of the initial specific flux (0.0029 gfd/psi). The hydraulic conditions were not optimized in this test, as the cartridge was operated in semicontinuous mode with only the draw solution tangentially flowing across the membrane surface. If the same cross-flow conditions could be achieved on both sides of the membrane, more turbulence would be created and the water transfer and specific flux would be greatly enhanced.
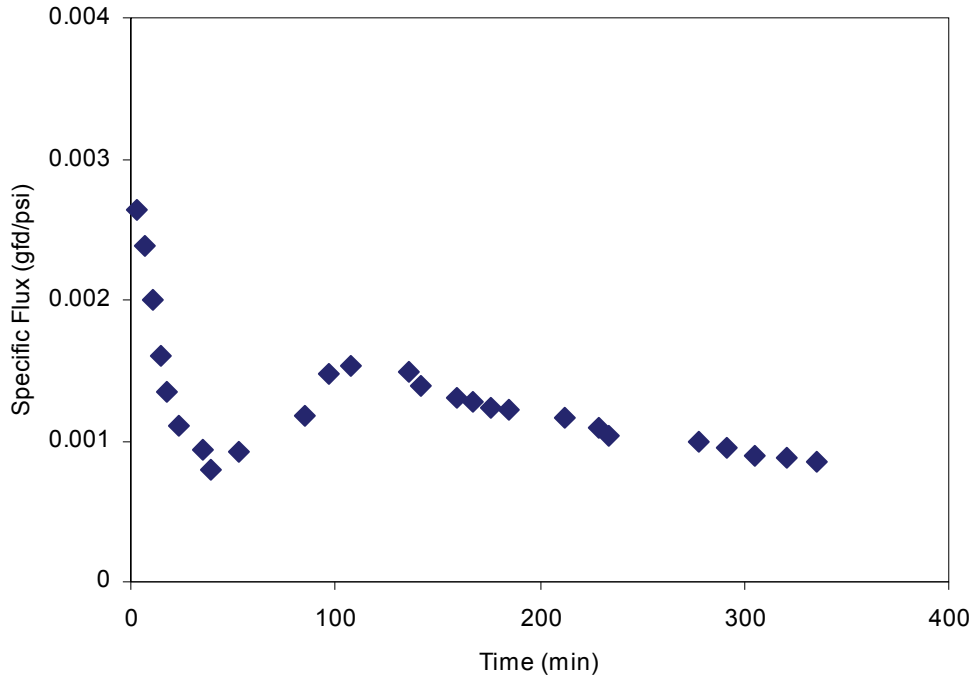
Figure 3.18. Change of specific flux with time in an FO cartridge with RO concentrate as the feed solution.

3.5 ECONOMIC EVALUATION RESULTS

In this study, the tests are conducted at the bench-scale level and data obtained from bench-scale studies are utilized to estimate the cost of the FO process.

Train 1 (Baseline Train): MBR/RO/ZLD
This train represents the baseline case for this economic evaluation (Figure 3.19). The costs for a Kubota MBR system were obtained from a previous study conducted on optimization of MBR systems (Adham et al., 2004). The RO costs were calculated by using a model developed by the research team (Adham and Kumar, 2004). The specific assumptions for the ZLD process were based on a recent reference (Mickley, 2001).

- o ZLD process considered consisted of a brine concentrator followed by a salt crystallizer as shown in Figure 3.19;
- o TDS limit in the brine concentrator was 300,000 mg/L;
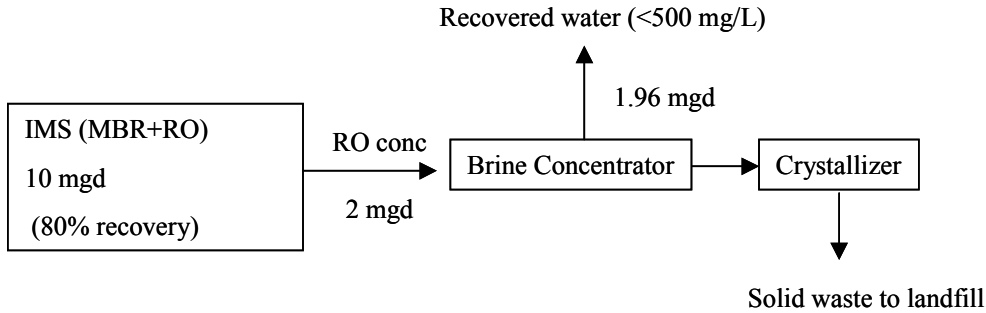- o Landfill disposal was assumed for the solid waste.

Recovered water (<500 mg/L)

1.96 mgd

| IMS (MBR+RO)

10 mgd

(80% recovery) | RO conc

2 mgd | Brine Concentrator | Crystallizer |

Solid waste to landfill

Figure 3.19. Process diagram of MBR-RO-ZLD system with assumptions.

Train 2 (FO Train): MBR/RO/FO/IX/ZLD
This train represents the use of FO for dewatering 2 mgd of the RO concentrate produced by the RO portion of the IMS train (Figure 3.20). The following assumptions were considered in estimating costs:

o The recovery for the FO process was assumed to be 70% based on the bench-scale testing results.
o The draw solution utilized for these tests was salt (NaCl). An NaCl concentration of 10% was found to be adequate.
o Membrane flux was considered as 2 gfd based on bench-scale testing results.
o NaCl was reconcentrated through the use of IX resin. This is particularly effective due to the absence of any interfering ions in the draw solution even after dewatering RO concentrate.
o IX was used to recover a portion of the draw solution stream (1.4 mgd), returning the balance (1 mgd) to be recycled back to the draw solution as shown in Figure 3.20. This stream will be mixed with the regenerant stream to restore the draw solution concentration to approximately 10%.
o The dewatered RO concentrate was sent to a ZLD process consisting of a brine concentrator and a crystallizer. Any assumptions mentioned in the ZLD process earlier were applied here.
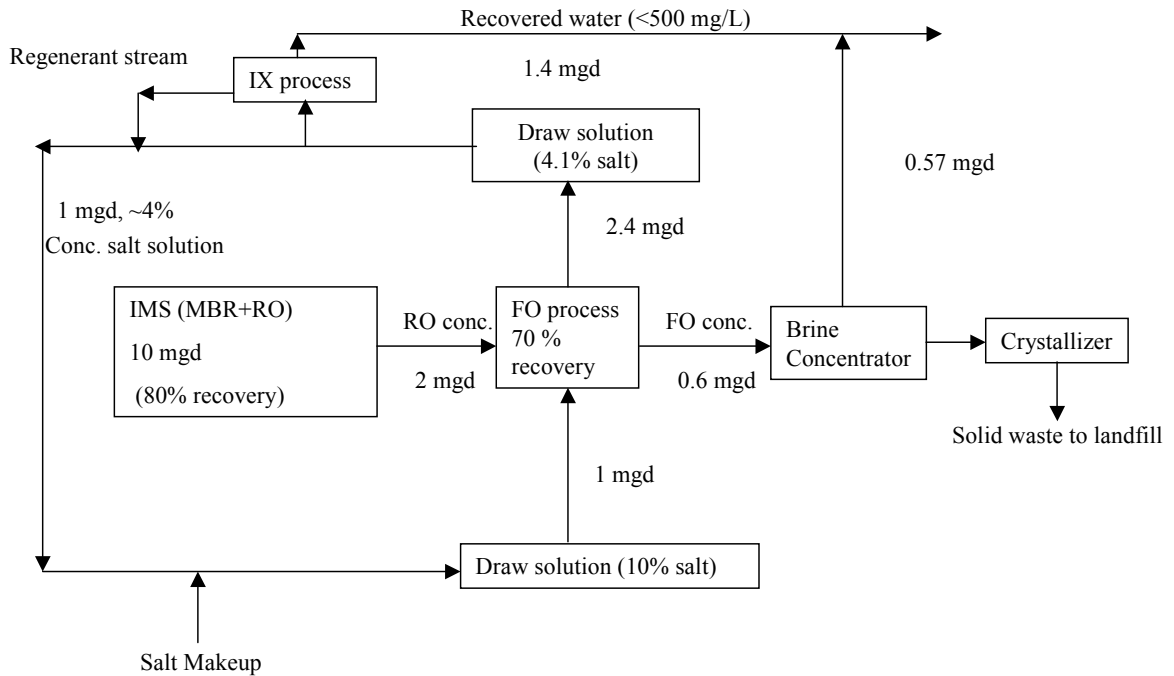
Figure 3.20. Process diagram of MBR-RO-FO-ZLD system with assumptions.

A comparison of the unit treatment costs for each train is shown in Figure 3.21. The overall cost of implementing FO for dewatering RO concentrate before ZLD processing is lower than that of implementing ZLD on the entire RO concentrate stream. The unit capital costs for the trains are similar ($1.86/1000 gal versus $1.88/1000 gal); however, there are substantial operational cost savings when utilizing the FO train ($2.49/1000 gal) rather than the baseline treatment train ($3.07/1000 gal). This indicates that FO could be a feasible process for reducing the costs of an integrated membrane treatment scheme by minimizing the volume of the RO concentrate requiring disposal.

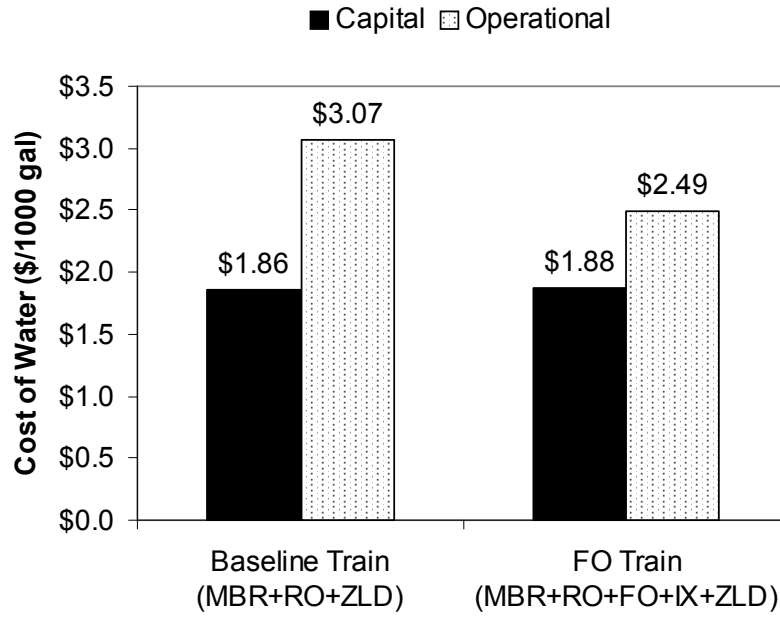**Figure 3.21. Comparison of unit costs for a 10-mgd integrated treatment train of incorporating the FO process for dewatering RO concentrate (FO train) before ZLD treatment and for a baseline train of utilizing the ZLD process for processing all the RO concentrate.**

CHAPTER 4

CONCLUSIONS AND RECOMMENDATIONS

4.1 CONCLUSIONS

The following conclusions can be drawn from this study on the use of FO to dewater RO concentrate. It should be kept in mind that it is an initial proof-of-concept study. Many of the ideas implemented in this project were tested for the first time, and hence attempts for optimization were kept to a minimum.

Evaluation of Innovative Draw Solutions
- o   A DCMO was designed to measure the osmotic pressures of innovative draw solutions such as magnetic nanoparticles and dendrimers. The osmotic performance of these compounds cannot be adequately predicted on the basis of theoretical calculations because of the uncertainty in the value of physical constants needed for the calculations. Actual osmotic pressure measurement through use of DCMO provided a basis for prediction of the performance of innovative draw solutions whose osmotic properties have not been well researched.

- o   The magnetic nanoparticles tested in this study did not provide high osmotic pressure for dewatering RO concentrate. This can be explained by the high molecular weight and low solubility of the nanoparticles. Our measurements, however, have shown that magnetic nanoparticles may have potential if they can be appropriately synthesized. If the nanoparticles can be designed to be smaller and less viscous and with a more hydrophilic surface, higher osmotic pressures may be obtainable.

- o   Dendrimers are a promising osmotic medium as these macromolecules provide high osmotic pressure. Twenty percent of G2-pentaearythrityl sodium carboxylate dendrimer solution provided 330 psi with its surface ions partially dissociated. UF has the potential to reconcentrate the dendrimer along with its surface ions. It was established that additional studies need to be conducted on the pH-controlled removal of specially designed dendrimers with ionizable surface groups and low buffering capacity.

- o   Salt (NaCl) has excellent properties as an osmotic agent, including low viscosity and high osmolality. In this study, salt was used as a baseline from which to design and evaluate real-world application of RO concentrate dewatering by FO.

Evaluation of FO Membranes
- o   Membrane B demonstrated the greatest osmotic permeability in the FO mode (specific flux of 0.0172 gfd/psi) out of all flat-sheet membranes tested in this study. It was identified as the best membrane and was used in bench-scale FO experiments of dewatering RO concentrate.

Bench-Scale FO to Dewater RO Concentrate
- o Bench-scale experiments have shown that the RO concentrate from an IMS pilot in Rio Rancho, NM, could be further concentrated by using FO. With the flat-sheet FO configuration, the volume of RO concentrate was reduced by 71% after 20 h of operation, achieving an overall recovery of 94% for the combined RO and FO processes. The precipitate that occurred in the FO process was mostly calcium (99.3%) with a small amount of silica (0.7%).

- o Softening the RO concentrate helped to remove the hardness and silica in the feed. The decline in specific flux was decreased by 8% under the tested softening conditions.

- o Low-pH cleansers could easily recover the permeability of a fouled FO membrane. In this study, a fouled membrane was cleaned with 2% citric acid (pH = 2.24) and the specific flux recovered to 81% of the initial specific flux.

Economic Evaluation
- o The FO process has been shown to be economically feasible for RO concentrate minimization. The costs for implementing FO for dewatering RO concentrate before ZLD processing are lower than those for implementing ZLD on the entire RO concentrate stream, as operational costs were substantially reduced by utilizing the FO train ($2.49/1000 gal) instead of the baseline treatment train ($3.07/1000 gal) for a 10-mgd IMS incorporating an MBR and an RO process. The use of salt as the draw solution and an IX process for reconcentrating the salt from the diluted draw solution was also found to be economically feasible.

4.2   RECOMMENDED FUTURE WORK

Investigation of Custom-Designed Dendrimers Allowing for Effective Reconcentration
The current study demonstrated that dendrimers are a promising osmotic medium as these macromolecules provide high osmotic pressure. Further research needs to be conducted to explore the recovery mechanisms of the dendrimer solution. One future direction is to test custom-designed dendrimers with ionizable surface ions and low buffering capacity. pH-controlled UF could be a potential method of reconcentrating dendrimers along with its surface ions.

Investigation of Custom-Designed Magnetic Particles for High Osmotic Potential
Magnetic nanoparticles may have the potential to be a good draw solution if they can be appropriately synthesized to be smaller and less viscous and with a more hydrophilic surface. Further research could be performed to explore custom-designed magnetic particles with these properties and their separation by using a gradient magnetic field.

Optimization of the FO Process at Bench Scale Prior to Pilot Testing
This study has demonstrated that the FO process is technically feasible for dewatering RO concentrate at bench scale. However, several operational issues such as FO cross-flow velocity, membrane orientation, draw solution concentration, optimized pretreatment, and cleaning procedure need to be explored further prior to scale-up.

Demonstration of the Application of Using FO to Dewater RO Concentrate at Pilot Scale

The FO process shows promise in minimizing the volume of RO concentrate, and a preliminary economic evaluation of this process suggests potential commercial value in applying the process. However, these studies were conducted in short-duration bench-scale tests, so the application of those technologies from bench scale to full scale will encounter scale-up operational challenges. It is therefore recommended that the FO process be demonstrated at the pilot scale in continuous operation as compared to batch operation.

REFERENCES

Adham, S.; Burbano, A.; Chiu, K.; Kumar, M. *Development of a Reverse Osmosis/Nanofiltration (Ro/Nf) Knowledge Base: Final Report;* Desalination Research and Innovation Partnership Project (DRIP), March 2005.

Adham, S.; DeCarolis, J. F.; Pearce, W. *Optimization of Various MBR Systems for Water Reclamation—Phase III;* Desalination Water Purification Research and Development Program Report No. 103; U.S. Bureau of Reclamation, U.S. Government Printing Office: Washington, DC, 2004.

Adham, S.; Kumar, M. *Cost of Salt Removal from Various Waters with Membrane Systems: Final Report;* Desalination Research and Innovation Partnership Project (DRIP), 2004.

AWWA. *Water Desalting Planning Guide for Water Utilities.* John Wiley & Sons, Inc.: Hoboken, NJ, 2004.

Cath, T. Membrane Contactor Processes for Seawater Desalination and Wastewater Reclamation. Ph.D. Thesis, University of Nevada, Reno, 2004.

Cath, T. Y.; Childress, A. E.; Elimelech, M. Forward osmosis: principles, applications, and recent developments. *J. Membr. Sci.* **2006,** *281,* 70–87.

Chahine, N. O.; Chen, F. H.; Hung, C. T.; Ateshian, G. A. Direct measurement of osmotic pressure of glycosaminoglycan solutions by membrane osmometry at room temperature. *Biophys. J.* **2005,** *89,* 1543–1550.

Cohen, D. http://www.chemicalprocessing.com/articles/2004/346.html (accessed April 2007).

Cohen, J. A.; Highsmith, S. An improved fit to website osmotic pressure data. *Biophys. J.* **1997,** *73,* 1689–1694.

Dendritic Nanotechnology, Inc. *Product Catalog;* http://dnanotech.com (accessed April 2007.)

Diallo, M. S.; Christie, S.; Swaminathan, P; Johnson, J. H.; Goddard, W. A. Dendrimer enhanced ultrafiltration. 1. Recovery of Cu(II) from aqueous solutions using PAMAM dendrimers with ethylene diamine core and terminal NH_2 groups. *Environ. Sci. Technol.* **2005,** *39,* 1366–1377.

Kestin, J.; Shankland, L. Viscosity of aqueous NaCl solutions in the temperature range 25–200 °C and in the pressure range 0.1–30 MPa. *Int. J. Thermophys.* **1984,** *5,* 241–263.

McCutcheon, J. R.; McGinnis, R. L.; Elimelech, M. A novel ammonia-carbon dioxide forward (direct) osmosis desalination process. *Desalination* **2005,** *174*, 1–11.

McCutcheon, J. R.; McGinnis, R. L.; Elimelech, M. Desalination by a novel ammonia-carbon dioxide forward osmosis process: influence of draw and feed solution concentrations on process performance. *J. Membr. Sci.* **2006,** *278,* 114–123.

McGinnis, R. L. Osmotic desalination process. U.S. Patent 6,391,205, May 21, 2002.

Mickley, M. C. *Membrane Concentrate Disposal: Practices and Regulations;* Desalination and Water Purification Research and Development Report No. 69; U.S. Department of

the Interior, Bureau of Reclamation, U.S. Government Printing Office: Washington, DC, 2001.

Moeser, G. D.; Roach, K. A.; Green, W. H.; Hatton, T. A.; Laibinis, P. E. High-gradient magnetic separation of coated magnetic nanoparticles. *AIChE J.* **2004,** *50,* 2835–2848.

MWH. *Water Treatment: Principles and Design*, 2nd ed. John Wiley & Sons, Inc.: Hoboken, NJ, 2005.

MWH. *Evaluation of Minimization and Beneficial Reuse Options for Integrated Membrane Process Residuals;* Report submitted to Sandia National Laboratories: March 2006.

Osmotek, Inc. *Landfill Leachate Treatment;* http://www.rimnetics.com/osmotekmenu.htm (accessed April 2007).

Pankhurst, Q. A.; Connolly, J.; Jones, S. K.; Dobson, J. Applications of magnetic nanoparticles in biomedicine. *J. Phys. D: Appl. Phys.* **2003,** *36,* 167–181.

Petrotos, K. B.; Quantick, P. ; Petropakis, H. A study of the direct osmotic concentration of tomato juice in tubular membrane–module configuration. The effect of certain basic process parameters on the process performance. *J. Membr. Sci.* **1998,** *150,* 99–110.

Scatchard, G.; Batchelder, A.; Brown, A. Chemical, clinical, and immunological studies on the products of human plasma fractionation. VI. The osmotic pressure of plasma and of serum albumin. *J. Clin. Invest.* **1944,** *23,* 458–464.

Singh-Zocchi, M.; Andreasen, A.; Zocchi, G. Osmotic pressure contribution of albumin to colloidal interactions. *Biophysics* **1999,** *96,* 6711–6715.

Tomalia, D. A.; et al. A new class of polymers: starburst dendritic macromolecules. *Polym. J.* **1985,** *17,* 117–132.

Tu, R. S.; Breedveld, V. Microrheological detection of protein unfolding. *Phys. Rev. E: Stat. Nonlin. Soft Matter Phys.* **2005,** *72,* 041914.

Wangnick, K. *IDA Worldwide Desalting Plants Inventory;* Report No. 18; Wangnick Consulting GMBH: Gnarrenburg, Germany, 2004.

York, R. J.; Thiel, R. S.; Beaudry, E. G. *Full-Scale Experience of Direct Osmosis Concentration Applied to Leachate Management;* Proceedings of the Sardinia '99 Seventh International Waste Management and Landfill Symposium, S. Margherita di Pula, Cagliari, Sardinia, Italy, 1999.

Advancing the Science of Water Reuse and Desalination

WATEREUSE
FOUNDATION